TECHNOLOGY TRENDS ASSESSMENT

ISO/TTA 5

Second edition
2007-10-15

Code of practice for creep/fatigue testing of cracked components

Code de bonne pratique pour les essais de fluage/fatigue des composants fissurés

Reference number
ISO/TTA 5:2007(E)

ISO copyright office
Case postale 56 • CH-1211 Geneva 20
Tel. + 41 22 749 01 11
Fax + 41 22 749 09 47
E-mail copyright@iso.org
Web www.iso.org

Published in Switzerland

Foreword

ISO (the International Organization for Standardization) is a worldwide federation of national standards bodies (ISO member bodies). The work of preparing International Standards is normally carried out through ISO technical committees. Each member body interested in a subject for which a technical committee has been established has the right to be represented on that committee. International organizations, governmental and non-governmental, in liaison with ISO, also take part in the work. ISO collaborates closely with the International Electrotechnical Commission (IEC) on all matters of electrotechnical standardization.

International Standards are drafted in accordance with the rules given in the ISO/IEC Directives, Part 2.

The main task of technical committees is to prepare International Standards. Draft International Standards adopted by the technical committees are circulated to the member bodies for voting. Publication as an International Standard requires approval by at least 75 % of the member bodies casting a vote.

To respond to the need for global collaboration on standardization questions at early stages of technological innovation, the ISO Council, following recommendations of the ISO/IEC Presidents' Advisory Board on Technological Trends, decided to establish a new series of ISO publications named 'Technology Trends Assessments' (ISO/TTA). These publications are the results of either direct cooperation with prestandardization organizations or ad hoc Workshops of experts concemed with standardization needs and trends in emerging fields.

Technology Trends Assessments are thus the result of prestandardization work or research. As a condition of publication by ISO, ISO/TTAs shall not conflict with existing International Standards or draft International Standards (DIS), but shall contain information that would normally form the basis of standardization. ISO has decided to publish such documents to promote the harmonization of the objectives of ongoing prestandardization work with those of new initiatives in the Research and Development environment. It is intended that these publications will contribute towards rationalization of technological choice prior to market entry. Whilst ISO/TTAs are not Standards, it is intended that they will be able to be used as a basis for standards development in the future by the various existing standards agencies.

Attention is drawn to the possibility that some of the elements of this document may be the subject of patent rights. ISO shall not be held responsible for identifying any or all such patent rights.

ISO/TTA 5 was prepared by VAMAS TWA25 and published under a memorandum of understanding concluded between ISO and VAMAS.

This second edition cancels and replaces the first edition (ISO/TTA 5:2006), which has been technically revised.

Contents

Page

Code of practice for creep/fatigue testing of cracked components

1 EXECUTIVE SUMMARY

Following a brief description of the mechanism for creep and creep/fatigue this document details testing methods and analysis procedures needed for creep and creep/fatigue crack growth testing of generic geometries containing cracks. Use of the terms 'generic geometries', 'component' or 'feature component', 'feature specimens' in testing assumes that the test geometry is non-standard as compared to standard laboratory fracture mechanics geometry such as the Compact Tension (C(T)). These tests maybe needed when the users need additional validation of results and in cases where excessive costs, unavailability of pedigree material, and other testing constraints would allow nominal numbers of tests can be carried out. So far as available, specific advice and additional reference material is given throughout the document in order to assist the user in carrying out a programme of testing and analysis of the data. Specific geometries are identified and appropriate fracture mechanics parameters are presented for each of them.

This document takes into account the experience gained in testing techniques from previous Standards and Codes of Practice [[a]-[kk]] and integrates early advances in the field of high temperature fracture mechanics [1-23] with the more recent findings [24-80] to give advice on testing, measurement and analysis of CCI, CCG and CFCG data for a range of creep brittle to creep ductile materials using a very wide range of pre-cracked geometries. In quantitative terms the information from these tests can be used to consider the individual and combined effects of metallurgical, fabrication, operating temperature, and loading variables on creep crack growth life of a component.

This document, by the very nature of the subject's diversity, cannot go into detail on every issue relating to the methods of testing and the type of geometry that could be tested. Rather it identifies common grounds in the procedures and highlights the sensitivity of the various parameters in completing a validated programme to derive material 'basis' data. Attempts have been made to simplify the procedures whilst at the same time not compromise the overall accuracy that is required in a test programme. Finally advice and recommendations are given to identify the limitations of test results and/or analysis for any specific condition.

2 SCOPE

The scope of this document is to recommend and establish standardized techniques for measuring and analysing Creep Crack Initiation (CCI), Creep Crack Growth (CCG), and Creep Fatigue Crack Growth (CFCG) characteristics using a wide range of pre-cracked standard and non-standard 'feature' geometries. Specimens considered in this document are shown in APPENDIX I. The list of geometries is not by any means complete and the user is advised to use appropriate information from other databases for other geometries to derive the relevant fracture mechanics parameters (see Section **11**) to use in the analysis. The validation of the parameters that are to be used however is important,

especially where concern exists regarding the compatibility of test geometry with the actual component in terms of size, the type of loading and stress state. This document allows increased flexibility and a wider choice of geometries than previously were made available without comprising on the important issues such as accuracy of testing and data measurements and the appropriate derivation of the correlating parameter. Less emphasis and detail has been placed on cycle dependent fatigue test methods compared to time dependent creep test methods as fatigue testing has been comprehensively dealt with in other standards [g] and the parameters needed for its analysis are linear elastic in nature and therefore simpler than the non-linear time dependent creep regime.

3 SPECIFIC OBJECTIVES

Availability of Creep Crack Initiation (CCI) and Creep Crack Growth (CCG) and Creep/Fatigue Crack Growth (CFCG) properties are essential for defect assessments of components operating at elevated temperatures. Methods for deriving the uniaxial creep properties are well established. The following identifies the specific objectives for this CoP

1 The user is given advice and information on specific test geometries, techniques, testing methods to allow obtain the maximum amount of verifiable test information for creep and creep/fatigue tests.
2 The information presented has been derived from collaborative experiments on a range of geometries forming the basis for the validation of results in this CoP.
3 Maximum flexibility has been introduced in test techniques without compromising accuracy. Hence the advice will also be relevant to geometries that are not identified specifically in the appendices
4 Advice is given on specimen selection and the appropriateness of fracture mechanics parameters for use in the analysis taking into account the creep properties of the material.
5 Without compromising overall accuracy simplifications of parameters have been introduced and the appropriate variability due to the method of analysis is estimated.
6 The results for the geometries listed in APPENDIX I have been compared and validated and the analysis methods standardized so that testing variability between different laboratories can be reduced to a minimum.
7 The CoP sets out to identify the commonality in the wide variety tests and provides the user with sufficient advice to devise, carry out and analyse a test.

In effect the overall objective of this CoP is to unify, as far as possible, testing and analysis methods between different laboratories. This is in order that subsequent or future analysis of the data or its use in life assessment analysis could be performed with confidence and increased overall accuracy.

4 INTRODUCTION

The Versailles Project on Advanced Materials and Standards (VAMAS) supports trade in high technology products through International collaborative projects aimed at providing the technical basis for drafting codes of practice and specifications for advanced materials. The scope of the collaboration embraces all agreed aspects of enabling science and technology which are required as a precursor to the drafting of standards for advanced materials. The VAMAS activity emphasizes collaboration on pre-standards measurement research, inter-comparison of test results, and consolidation of existing views on priorities for standardization action.

4.1 Background to VAMAS Creep Crack Growth Initiatives

At this point it is useful to outline the background to the development of this document as it will place it in context with the already available codes and standards related to this subject.

VAMAS has been active in the field of standardisation of testing and analysis of elevated temperatures fracture mechanics specimens since 1987. A working group, TWA 11, was setup in 1987-1992 to develop and formulate a standard for a high temperature test method. This involved making recommendations for measuring the creep crack growth properties of materials and using the creep fracture mechanics parameter C^* in the analysis of the data. The method was restricted to creep-ductile cracking conditions. The findings were incorporated into ASTM test procedure E1457-92 [i] that was the first standard to deal with crack growth testing at elevated temperatures.

This methodology was extended under TWA 19 (1993-1998) to conditions where only limited creep deformation or otherwise creep brittle conditions were observed. As a consequence of a Round Robin testing and analysis programme on four relatively creep brittle alloys, namely two aluminium a titanium and a carbon-manganese alloy, recommendations were made to change the original testing procedure, to incorporate the methodology for a more creep brittle circumstances. The findings of TWA19 were published in a special issue of Engineering Fracture Mechanics [11]. Subsequently a revised version of the ASTM testing standards E1457-01 [i] was published. This edition covers the wider range of creep ductile to creep brittle testing conditions observed in engineering alloys.

Following these earlier developments it has become evident recently that industry needs additional justifications and verifications in order to apply the standard test data with confidence in present component defect assessment codes such as R5 [29-31], A16 [32-33], BS-7910 [34] and API 579 [35]. As a result of experience gained from TWA 11 and TWA 19 the present TWA 25 was established in June.

4.2 Background to Industrial needs for validated Test Data

Manufacturer's recommendations and their past experience have usually been the basis for the design of vital engine components such as turbine blades, vanes and discs and in critical engineering components such as gas steam pipes, pressure vessels and in weldments which might contain pre-existing defects. In recent times however crack growth initiation and failure analyses have become more acceptable as an independent design and remaining life assessment methodology. The development of high temperature fracture mechanics concepts, through which the time dependent effects of creep could be modeled, uses experimental uniaxial and crack growth data from simple laboratory tests specimens in order to predict failure times under operating conditions. Furthermore the improvement in non-destructive inspections and testing methods (NDT) has allowed smaller and smaller defects to be detected and the need for more reliable methods for predicting crack initiation/incubation periods and steady crack growth rates.

Figure 1 shows a schematic of the overall relationship between testing and component assessment showing the circular link between developing test methods and applying it to life assessment which in turn feeds information back into improving testing methods. The main objective of developing testing procedures is to improve the reliability of design and life assessment codes, which use material basis data for their calculations. In developing a testing standard methodology for laboratory specimens a first step was taken to improve life prediction procedures of components. However life extension calculations of components requires a validated fracture mechanics model for crack initiation and growth as well as detailed knowledge of component non-linear time dependent stress analysis, past service records and postulated future operations together with 'appropriate' mechanical

properties. It therefore seemed appropriate to develop a testing method for components and integrate it with life assessment codes for creep and creep/fatigue of components.

4.3 Relevance of Testing Methods to Life Assessment Codes

4.3.1 *Background to Life Assessment Codes*

Components in the power generation and petro-chemical industry operating at high temperatures are almost invariably submitted to static and/or combined cycle loading. They may fail by net section rupture, crack growth or a combination of both. The development of codes in different countries has moved in similar direction and in many cases the methodology has been borrowed from a previously available code in another country. The early approaches to high temperature life assessment used methodologies that were based on defect-free assessment codes. For example ASME Code Case N-47 [36] and the French RCC-MR [37], which have many similarities, are based on lifetime assessment of un-cracked structures. The materials properties data that are used for these codes is usually uniaxial properties and S-N curves for fatigue.

More recent methods make life assessments based on the presence of defects in the component. The codes dealing with defects [31-35] vary in the extent of the range of failure behaviour they cover. Essentially fracture mechanics solutions dealing creep and creep/fatigue interaction in initiation and growth of defects are covered. In terms of creep crack growth all propose similar approaches but use different formulae which is likely to affect the predictive solutions. In such codes material properties, dealing with crack growth data that are needed are more complex compared to uniaxial data both in terms of testing methods and derivation.

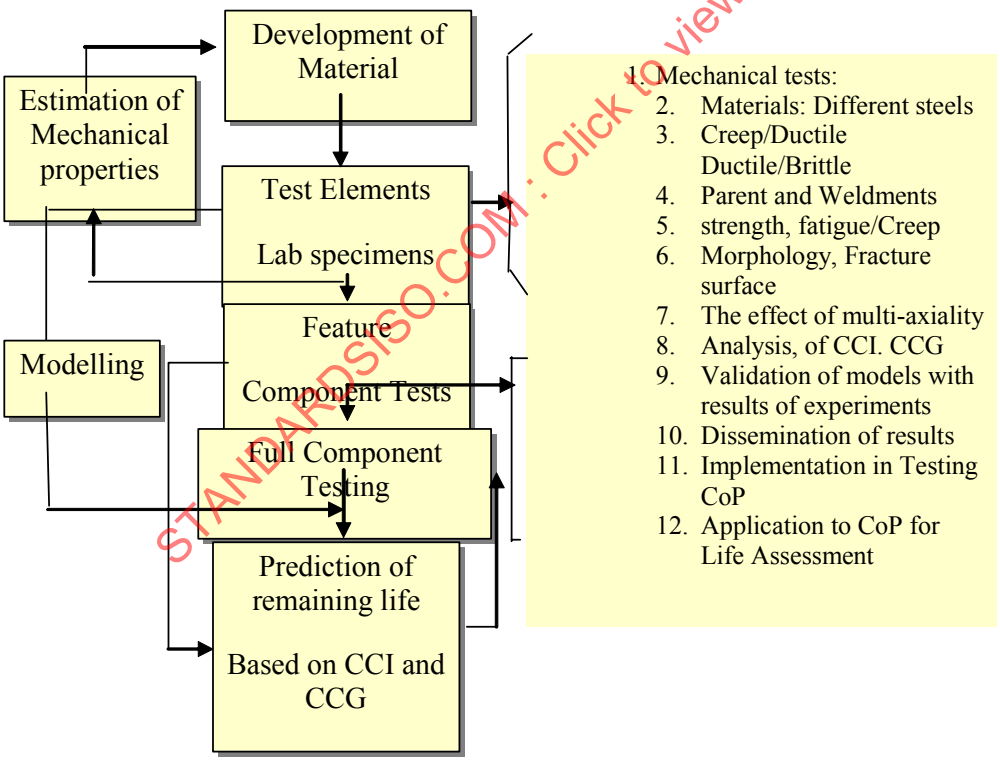

Figure 1: Schematic of the objectives in high temperature testing procedures.

4.3.2 *Relation between laboratory tests and Component Assessment Codes*

Generally defect assessment problems can be divided into two regions. Firstly the initiation region whose limit can be determined either from micro-mechanical models or from NDT limits and secondly the steady crack growth region which can be described using the fracture mechanics parameters such as K, reference stress σ_{ref} and C^*. The more recent defect assessment procedures mentioned above are based on experimental and analytical models to assess crack initiation and growth and to determine the remaining useful life of such components. These codes base their analysis on tests taken from laboratory specimens, which are invariably derived from small specimens at short test times. Therefore there is no direct verification of the predicted results with component tests or behaviour. This is an important point since size and geometry differences impose various degrees of constraint [25], which affects crack growth and initiation. Furthermore the development of residual stresses during fabrication and loading history which may be non-existent in small laboratory testing will need to be considered for components.

In addition it is clear from these assessment methods that the correct evaluation of the relevant fracture mechanics parameters, for which the lifetime prediction times are dependent upon, are extremely important. It is also evident that the detailed calculation steps, which are proposed in these documents, do not in themselves improve the accuracy of the life prediction results. In any event as these procedures have been validated for limited sets of geometries and material data their use in other operating conditions will need careful checking.

The codes [31-35] attempt to deal comprehensively with assessment and remaining life estimation procedures that can be used at the design stage and for in service situations. The Codes' approach allows the expert to make decisions based on predictions made using the methodology in relation to the operating circumstances of the component. The concept implies that the codes need to show they are both reliable and understandable over a range of material and loading conditions that may not have been previously examined or validated by the code developer. This is particularly important as new higher strength steels, which have little or no long-term material properties database, are developed or used by the power industry.

4.3.3 *Factors involved in the development of assessment codes*

Figure 1 highlights the importance of research in the improvement and extension of industrial codes. The trend in the development of the codes suggests that, in addition to verification of data between laboratory tests and component tests the following factors need to be considered

1. The available material property data for the analysis is invariably insufficient or crude and since they are usually taken from either historical data, results from different batches of material or tested in different laboratories with insufficient number of tests specimens they are likely to contain a large scatter.
2. The scatter and sensitivity in creep properties inherently produce a large variation in the calculations. Upper and lower bounds are therefore introduced which give widely different life prediction results.
3. Improvements in the evaluation of the relevant parameters such as K, limit load concepts, reference stress σ_{ref} and C^* since they can be very different according to the method of derivation. Use of 3D non-linear FE methods would help in this task.
4. The uses of short-term small laboratory data for use in long-term component life predictions further increases the possibilities of a wrong prediction. The relationship between short and long term behaviour needs to be quantified.

5. Difficulty in ascertaining the level of crack tip constraint and multiaxiality effects in the component could reduce the accuracy of crack growth predictions, in the extreme, by about a factor of 30. Use of 3D FE modeling would assist in this task.
6. Unknowns in modeling the actual loading history, component system stresses and additional unknowns such as little or no knowledge of past service history, residual stresses also act as sources of error in predictions.
7. Non-destructive examination methods (NDE) of measuring defects in components, during operation and/or shutdown and insufficient crack measurement data during operation, are likely to add to errors involved in life-time assessment.
8. Probabilistic assessment of data and the predictions are required to deal with the material properties sensitivity to the models, test data scatter and unknowns in the parameters and predictive models.

Furthermore similarities of the approaches in the various codes do not necessarily imply that calculations by the different methods will give the same predictions. It may be possible that under certain controlled and validated circumstance the predictions can be optimized. It is clear that a critical comparison is only possible when the same method is used on another material and condition or the same test cases are examined by the different codes.

4.4 Requirements for the VAMAS TWA 25 CoP

The international project, under the auspices of VAMAS (Versailles Agreement on Advanced Materials and Standards), Technical Working Area 25 (TWA 25) was initiated in June 1999. The broad was for the committee to recommend testing, analysis and life prediction methods for assessing elevated temperature creep and creep/fatigue crack growth in metallic components containing defects and to carry out and gather together the under-pinning and pre-standard research necessary to develop a standard. The investigation involved the collaboration of a number of industrial and research establishments (see Section [5]). The work followed the already established high temperature testing methodology of standard specimens developed previously by the VAMAS TWA11 (1988-92) and TWA19 (1993-1998) committees. The information from these studies, the work performed by ASTM E08 Creep Crack Growth Committee and a number of collaborative EU (BRITE/EURAM) projects based on high temperature crack growth (see Section 5, acknowledgements) was used in TWA25 to develop this document. Some of the results have been published previously in a special issue of the International Journal of Pressure Vessel and piping [24]. In addition to the input from partners' information from historical work plus results form the more recent work found in the literature has also been used in the development of this Code of Practice (CoP). The comprehensive review was performed in order to validate the testing and analysis procedures and give practical advice to the user of this document.

This document therefore reports the findings of a comprehensive study which was carried out by the VAMAS Technical Working Area TWA 25 to investigate methods for testing non-standard pre-cracked components under static and cyclic loading at elevated temperatures. This document is aimed at demonstrating the methodology in testing procedures and the subsequent analysis of the reported data. The document has been set out in such a way that it would be possible to expand it in future updates to take account of new information and data.

4.5 ISO requirements

ISO (the International Organization for Standardization) is a worldwide federation of national standards bodies (ISO member bodies). The work of preparing International Standards is normally carried out through ISO technical committees. Each member body interested in a subject for which a

technical committee has been established has the right to be represented on that committee. International organizations, governmental and non-governmental, in liaison with ISO, also take part in the work.

International Standards are drafted in accordance with the rules given in the ISO/IEC Directives, Part 2. The main task of technical committees is to prepare International Standards. Draft International Standards adopted by the technical committees are circulated to the member bodies for voting. Publication as an International Standard requires approval by at least 75 % of the member bodies casting a vote.

4.5.1 *ISO Technology Trend Assessment (ISO/TTA)*

(ISO/TTA) documents are published under a memorandum of understanding concluded between ISO and VAMAS. They enable the technical innovations and developments emerging from a VAMAS activity to be published at an early stage prior to their incorporation into a Standard. Whilst ISO/TTAs are not Standards, it is intended that they will be able to be used as a basis for standards development in the future by the various existing standards agencies.

5 Acknowledgements

This Code of Practice has been prepared with help provided by the VAMAS TWA25 [1999-2005] project partners core group listed below in Section 5.1. Additional information has come from the ASTM E08, ESIS TC11 and previous VAMAS TWA 11 and 19 committees as well as from four European Union sponsored projects called

1. 'CCG in CMn', EU Project, 1993-1997, 'CCG in Carbon-Manganese at 320-400'
2. 'HIDA', EU Project, 1996-2000, 'High Temperature Defect Assessment'
3. 'LICON', EU Project, 1997-2001, 'Accelerated Test Methods for Advanced Steels'
4. 'CRETE', EU Project 2001-2004, 'Creep Crack Growth Testing for an EU CoP'

5.1 List of participants in VAMAS TWS25

1. *Teikyo University, Japan*
2. *British Energy Generation Ltd., UK*
3. *Tohoku University, Sendai, Japan*
4. *NIMS, Tsukuba, Japan*
5. *IHI, Yokohama, Japan*
6. *GKSS- Geestacht, Germany*
7. *University of Arkensas, USA*
8. *Bristol University, UK*
9. *Imperial College, UK*
10. *Alsthom, UK*
11. *Boeing, Huntingdon-USA*
12. *KAERI-South Korea*
13. *MPA, Germany*
14. *TUD, Germany*
15. *SPG, Germany*
16. *VTT, Finland*
17. *Wright-Patterson AFB- Dayton.USA*
18. *PVRC- , New York, USA*
19. *CEA, France*
20. *CETIM, France*
21. *ETD, UK*

6 NOMENCLATURE AND ABBREVIATIONS

6.1 Nomenclatures

A, H, D_o, m, p. φ	Various material constants described in appropriate Equations
$E' = E/(1-\nu^2)$	for plane strain and E for plane stress where, E= elastic modulus (GPa)
ν	Poisson's ratio
P, P_L, M_L	applied load (MN), limit load (MN), limit moment (N/m)
P_{max}, P_{min}	maximum Load (MN), minimum load (MN)
p	pressure (MPa)
R	load ratio P_{min} / P_{max}
$\dot{\varepsilon}$, $\dot{\varepsilon}_{min}$, $\dot{\varepsilon}_{Ave}$	creep strain rate, minimum and average creep strain rates
a, a_i, a_f	crack length (mm), initial crack length (mm), final crack length (mm)
da/dt or	creep crack growth rate (mm/h)
Δa_i, Δa_f	initial crack extension (mm), total crack extension (mm)
t, t_Δ, t_i	test time (h), time increment (h), time to initiation
$\dot{a}_i$, $\dot{a}_s$	initial transient and steady state creep crack growth rate (mm/h)
$\Delta^t, \Delta^p, \Delta^c, \Delta^e$	Components of total, plastic, creep and elastic displacements
$\Delta^{LLD}, \Delta^{CMOD}$	load-line LLD and crack mouth opening CMOD displacements
$d\Delta^p/dt$ or $\dot{\Delta}^p$	plastic load-line displacement rate (mm/h)
$d\Delta^c/dt$ or $\dot{\Delta}^c$	creep load-line displacement rate (mm/h)
$d\Delta^e/dt$ or $\dot{\Delta}^e$	elastic load-line displacement rate (mm/h)
$d\Delta^\tau/dt$ or $\dot{\Delta}^t$	total load-line displacement rate (mm/h)
K, ΔK	stress intensity factor (MPa$\sqrt{m}$), stress intensity factor range (MPa$\sqrt{m}$)
J_p	fully-plastic contribution to J-integral
$C^*(t)$	transient value of C^* (MJ/m^2.h)
C^*	steady state NLEFM creep correlating parameter (MJ/m^2.h)
ϕ, D	power index and material constant in $da/dt = DC^{*\phi}$
ϕ_I, D_i	constant for CCI versus C^* in $t_i = D_i C^{*\phi i}$
n, A	Norton's creep index and material constant in $\dot{\varepsilon} = A\sigma^n$
m', A'	crack growth rate index and material constant in $da/dt = A'K^{m'}$
K^c_{mat}	creep toughness parameter (MPa$\sqrt{m}$)
Q^*	Parameter based on creep activation energy and local crack tip stress
N, da/dN	Number of load cycles, fatigue crack growth per cycle (mm/cycle)
c', C'	fatigue crack growth rate index and material constant in $da/dN = C'\Delta K^{c'}$
σ, σ_y	stress and normalized yield stress (MPa)
$\dot{\varepsilon}_{ref}$, σ_{ref}	creep strain rate at reference stress, reference stress (MPa)
Vi, V_f	initial and final values of the PD signal (mV)
R_i, R_e	internal and external radii of cylinder
Z	geometry factor
R_i, R_o	inner radius (mm), outer radius (mm)
m	yield load ratio

M	bending moment (N/m)
W	width (mm)
B, B_n	thickness (mm), net thickness (of a side-grooved geometry) (mm)
H	height (mm)
R_a , R_m	radius to notch root (mm), mean radius (mm)
Bate	function of dimensions
c, c_{ini}, c_{fin}	half-length, initial and final half-lengths of surface crack
SD	Standard deviation
Q	Activation Energy
R	Gas Constant
T	Absolute Testing Temp.

The values stated in SI units are to be regarded as the standard.

6.2 Listing of abbreviations

CoP	Code of Practice
CCG	Creep Crack Growth
CCI	Creep Crack Initiation
FCG	Fatigue Crack Growth
CFCG	Creep Fatigue Crack Growth
LEFM	Linear Elastic Fracture Mechanics
NLEFM	Non- Linear Elastic Fracture Mechanics
X-weld	Cross Weld
HAZ	Heat Affected Zone
PD	Potential Drop
NDT/NDE	Non-Destructive Testing/Examination
LLD	Load-Line Displacement
CMOD	Crack Opening Displacement
CTOD	Crack Tip Opening Displacement
SD	Standard Deviation
EU	European Community
CCG in CMn	EU Project, 1993-1997, 'CCG in Carbon-Manganese at 320-400 ^{o}C'
HIDA	EU Project, 1996-2000, 'High Temperature Defect Assessment'
LICON	EU Project, 1997-2001,'Accelerated Test Methods for Advanced Steels'
CRETE	EU Project 2001-2004, 'Creep Crack Growth Testing for an EU CoP'
VAMAS	Versailles agreement on Materials and Standards
ASME	American Society of Mechanical Engineers
ASTM	American Society for Testing Materials
BSI	British Standards Institute
ISO	International Standards Organisation
FAD	Failure Analysis Diagram
TDFAD	Time Dependent Failure Analysis Diagram

7 DESCRIPTION OF CREEP AND FATIGUE CRACKING

7.1 Failure due Creep Crack Growth (CCG)

Failure due to creep cracking is usually identified by the intergranular separation of the grains. In creep ductile materials, extensive creep occurs when the entire uncracked ligament undergoes creep deformation. In the case of extensive creep, the region dominated by creep deformation is significant in size in comparison to the crack size and to the uncracked ligament size. In small-scale-creep or in creep brittle conditions only a small region of the uncracked ligament near the crack tip experiences creep deformation. The damage mechanism in both CCI and CCG are similar and for most practical circumstances may be correlated by the same parameters.

7.2 Creep Crack Initiation (CCI)

The early stages of growth are defined as initiation period or CCI and purely as a practical method a measurable distance is chosen which is usually linked to the limits of crack growth measurement sensitivity or NDE limits. This distance could range between 50 microns to as much as a few millimeters. In laboratory tests it has been established that 200 to 500 microns is generally measurable and therefore the period for CCI would cover this length scale and CCG would be the period beyond that length. Any variation in stress distribution from the transient to the steady state would also in the CCI region. In consideration of a number of factors such as specimen size, geometry and accuracy of measurements this CoP has adopted a crack extension of 0.5 mm set as the engineering limit for CCI (see Section 9.1).

7.3 Transient crack growth conditions

Transient crack growth conditions occur in the early stages of crack growth tests for the whole range of creep brittle/ductile behavior. It consists of a period when the elastic stress field transforms into the steady state C^* field ahead of the crack tip and also a period of creep damage development in which the crack tip creep strain overrides the initial elastic strain. The time to reach the latter is usually much greater than the former. This initial period usually constitutes a substantial portion of life of the specimen or the structure. CCI covers the transient period plus the period prior steady state CCG depending on the definition for CCI. CCI is identified as the time taken to reach a specific crack extension Δa_i. In 'Feature Component' testing where crack growth measurement sensitivity has been found to be lower 0.5 mm is the established CCI limit. This length is set as 0.2 mm or the limiting length of initial crack extension that can be safely measured using NDT. The limiting crack extension Δa_i should ideally not be set at > 0.5 mm in fracture mechanics testing. CCI can be correlated using C^* or K depending on material behaviour (see Section 9). The information derived from CCI can be used in applicable models to predict crack initiation times.

7.4 Steady state Creep Cracking (CCG)

Steady state CCG follows the transition period and the CCI period where a unique relationship will exist between CCG rate at steady state and C^* or K depending on the material behaviour (see Section 9). CCG is essentially derived from the measured crack extension versus time during a test. Methods for testing will be detailed in this Section. Steady-state creep crack growth rate behavior is usually used as the basic material property data for use in defect assessment analysis. The analysis details will be presented in Section 9.

7.5 Fatigue and Creep/Fatigue Crack Growth (FCG and CFCG)

These types of tests where loads are cycled at elevated temperatures are identified as FCG and CFCG tests depending on the frequency and R-Ratios used. It has been determined [20] that the analysis can generally be dealt with as fatigue dominant (FCG) at high frequencies (usually > 0.1 Hz) in FCG and as mainly time dependent creep (CFCG) at low frequencies (< 0.1 Hz). Therefore less emphasis and detail has been placed in this document for FCG test methods at high frequencies as fatigue testing at high frequencies is dealt with adequately in ASTM standard E647[g]. At low frequency elevated temperature cycling testing (CFCG) it is assumed that creep dominates and therefore the analysis can be in the same form as static loading tests.

7.5.1 *Failure due to fatigue*

Failure due to fatigue cracking at high frequencies (> 0.1 Hz) is usually identified by the transrgranular and at low frequencies (< 0.1 Hz) by intergranular separation of the grains. As opposed to CCG, FCG is a purely cycle dependant time independent phenomenon but CFCG is mainly time dependant. There are two regions of fatigue one is the threshold region where it is assumed that cracks will not grow below a threshold ΔK_{th} value for the stress intensity factor range and the steady state crack growth region which is usually described by the Paris Law $da/dN \propto K^{m'}$. However for CFCG tests no threshold exists as creep dominates the damage development at low frequencies. Also for life assessment purposes it is assumed that if there is fatigue loading there is no crack initiation period.

7.5.2 *Creep/Fatigue interaction*

Creep/Fatigue interaction comprises of cracking data derived from a cyclic test at elevated temperatures where creep mechanism for damage development is also prevalent. The effect on the total crack growth due to the combined actions of creep and fatigue will depend on the frequency, R-ratio and a number of other factors such as dwell periods and continuous cycling. As stated previously where the frequency is usually <0.1 Hz creep begins to dominate and where frequency is >1 Hz fatigue dominates. The region of maximum creep/fatigue interaction is found to be small ranging over 1 decade of frequency. Generally it has been shown that a linear cumulative crack growth addition of the creep and fatigue component can successfully be used, conservatively, to predict creep/fatigue interaction. This document adopts this methodology and Section 7 details the techniques for this analysis.

7.6 Factors affecting CCI, CCG and CFCG

There are number of factors which allow the development of cracks rather than the development of general damage and failure by rupture. As this procedure is mainly looking at cracking behaviour resulting from fracture mechanics tests it is useful to outline the important mechanisms which would dictate the choice of geometry for a test specimen.

7.6.1 *Creep properties*

Creep properties of materials as well as test geometries and their size have a profound effect on how CCI and CCG will develop in a specimen. The creep material properties are also extremely temperature sensitive in the creep range. Usually the component operating temperature dictates the range of test temperature that will be adopted for testing laboratory specimens. The level of creep ductility derived either as uniaxial creep failure strain, reduction area, or creep strain rate or stress sensitivity, usually quantified by the creep index n in Norton's creep equation or the shape of the uniaxial creep curve is used in developing appropriate CCI and CCG models [4,8,10]. The choice of test geometry, size and testing technique will need to address these factors before it is possible to

carry out a successful series of CCG tests. In Sections 9 the range of validities for the parameters in the creep brittle/ductile range are considered.

7.6.2 *Metallurgical effects*

Metallurgical effects on CCI and CCG can be significant where they affect the creep ductility of the structure. Generally the increased grain size increase creep embrittlement and induce sharp intergranular cracks. When test specimens are taken from regions of material that characteristically embody non-homogenous grain matrices. For example for directionally solidified alloys and single crystals, welds, X-welds and HAZ materials the testing techniques and the methods of analysis will in some cases be different to poly-crystalline materials. The choice and size of geometry for testing could be substantially affected. The use of the present procedure in these situations is acceptable so far as the user accepts the limitations and allows for it in the subsequent analysis of the data.

7.6.3 *Presence of residual stress fields*

Presence of residual stress fields in testpieces is another complication which can be addressed to a certain degree in this procedure. For example specimens can be taken out from weldments, and/or thick cast, forged, extruded products and product shapes where full stress relief is impractical. All such specimens could contain residual stresses. Extraction of specimens in itself partially relieves and redistributes the residual stress pattern; however, the remaining magnitude can still cause significant effects in the ensuing test. Distortion during specimen machining often indicates the presence of residual stresses. Residual stress is superimposed on applied stress and results in crack-tip stress intensity that is different from that based solely on externally applied forces or displacements. Furthermore relaxation of stresses during the test, which is likely to be a positive effect to slowing down CCG, will also add an added unknown. Depending on the extent and the compressive or tensile nature of the residual stress the relevant parameter that is used for the analysis of the data may deviate from that used in the homogenous material.

7.6.4 *Aggressive environments*

Aggressive environments at high temperatures can also significantly affect the CCI, CCG and CFCG behaviour. Once again by using the analysis methods for homogenous materials in non-aggressive environments are likely to give an overestimation and therefore appropriate safety factors should be employed. Where this information exists for a specific condition, this will be presented in this document. Otherwise the user should proceed with caution when analyzing the data in terms of C^*.

7.6.5 *Anisotropic and inhomogeneous material characteristics*

Variable material characteristics can be dealt with conveniently using the estimation method proposed in Section 12 for deriving C^*. Since C^* is effectively a measure of the rate of creep dissipation rate with respect to crack extension it can be assumed that variability in the material property will inherently be reflected as a measure of the load-line creep displacement rate. Therefore the energy interpretation for the derivation C^* should give an adequate correlation of the CCI, CCG and CFCG behaviour in the non-homogenous material conditions described above. Similarly the calculation of C^* using the reference stress method 9(shown in Section 12.2) should use the upperbound uniaxial creep strain rate properties taken from the weakest the region under consideration. In this way the calculated C^* will bee conservative reflecting the unknown nature of the inhomogeneity.

Note1: In all respects information should be fully logged for each test in order to identify diversions from the norm as specified in this CoP.

8 TEST METHODS

Detailed description of test techniques is presented in this Section which deals comprehensively with the all aspects of testing procedures. This advice covers the range of geometries and components describe in APPENDIX I section 13. It should be noted that under different conditions additional advice should be sought. However the accuracy limits detailed in this document should be adhered to.

8.1 Overview

The testing techniques and procedures are specified in this Section without being restrictive. Emphasis is placed on methods to carry out correct and repeatable testing procedures that will help to reduce scatter in the data and allow easier inter-laboratory comparisons to be made. The objectives in this Section are to present the techniques for testing and identify accuracy limits for measuring test variables. No insistence is placed upon the type of testing-rig, configuration and hardware/software for data collection to be used. Consequently the person performing the tests has been given the flexibility to configure the equipment in any way as long as the loading conditions and accuracy limits are maintained in accordance with the limits and conditions specified.

This Section will cover test methods for isotropic polycrystalline metallic materials. Where material inhomogeneity might exist, such as in testing single crystals, directionally solidified materials, variable grain size cast materials, welds, X-welds and Heat Affected Zone (HAZ) specimens the testing techniques are still applicable. However caution should be exercised in the treatment of the data and its analysis thereafter. Since the parameters described have been validated for homogenous material structures their use in inhomogeneous materials should proceed with caution. However it should be noted that for most instances this may be overcome by using appropriate safety factors. Therefore additional expert advice will be needed in these circumstances.

8.2 Test Geometries

The 'Benchmark' Compact Tension (C(T)) specimen is the most widely used geometry for creep and creep/fatigue testing. Available ASTM standard E1457 [i] have specifically adopted this geometry and have validated the parameters used in the analysis of the data. There are also, available, a substantial number of publications databases and information that have been gathered for this geometry. An indication of this can be found in the references listed [1-27]. Therefore any tests discussed here should ideally be compared with the proposed methods in ASTM E1457 [i] and ASTM E647 [g] standards. The 'benchmark' C(T) results if available would assist with the understanding and comparison of the cracking data resulting from geometric and size differences that may be encountered.

Two categories of test specimens are considered in this document all of which are identified as being of industrial interest for testing purposes. The first are the more widely used cracked geometries and are listed in APPENDIX I. The second categories of specimens are the 'feature' type specimens which are usually used to replicate, as near as possible, the actual component. These are listed in section 14.9. As previously stated the list is not a complete one. However they are the most common 'generic' type feature component (namely the 'Pipe' and the 'Plate' and solid notched bar geometries) that have been tested and their analysis validated [21,38-48]. The user is not restricted to the geometries described in APPENDIX I, Section 14.9. However the user must be in a position to be able to validate the functions employed to correlate the results obtained from other geometries since it is not within the scope of this CoP to cover every eventuality but rather to lay out a methodology.

For the geometries shown in APPENDIX I the definitions for the stress intensity factors K, C^* and reference stress solutions and associated functions are set out in the same APPENDIX I. The relevant merits and methods for their calculations and the applicability for the use of the parameters are discussed in Section 12.

8.3 Experimental Test Methods

Test methods for most cases of creep and creep/fatigue testing is in most cases universal. Therefore, this section covers wide ranging advice relevant to tests of different materials, geometries and loading conditions. APPENDIX V, Section 18, present further detailed advice on relevant testing and analysis techniques. Where the user finds insufficient advice for a particular case additional expert advice should be sought.

8.3.1 *Material procurement*

Material procurement either from new material or from service exposed or ex-service comes in many variations. Therefore detailed information of the material composition, pedigree, service-history (if any), heat-treatment and hardness should be logged. If possible a sample metallographic examination should be carried out to record the microstructure. Where available, mechanical properties should also be detailed at room and elevated temperatures.

8.3.2 *Specimen selection*

For all cases attention must be given to the proper selection of specimen. The choice of specimen should reflect a number of factors. These priorities can be listed as follows

-Availability and the size of material for testing

-Material creep ductility and stress sensitivity

-Capacity of the test rig

-Type of loading under consideration (tension, bending, tension/bending)

-Compatibility with size and stress state of the specimen with the component under investigation

-the number of specimens that can be tested

-the length and temperature of testing will dictate the size, initial crack length and side-grooving of the specimen.

It is likely that not all conditions can be satisfied at any one time. Therefore a compromise must be made by deciding what priorities are needed. This document goes part of the way to assist the user in this choice by identifying specific detail of a number of geometries. The appropriate decision may, however, need expert advice in the relevant field or industry.

8.3.3 *Crack-plane orientation*

Identification of the plane and direction of a crack growth test specimen in relation to product configuration should be made. This identification is designated by a hyphenated code with the first letter(s) representing the direction normal to the crack plane and the second letter(s) designating the expected direction of crack propagation (see Terminology E 1823 [k] for further discussion).

8.3.4 *Specimen machining*

Machining the specimens described within the specified tolerances is very important. The specimen dimensions shall be within the tolerances given in the figures shown in Appendices I and II. The direction and position of machined specimens should be logged. The final dimensions of the

machined specimen should be measured and the direction and position of specimen extraction should be noted. The choice of specimen size and thickness is flexible to the extent that the geometric ratios should be adhered to. Care should be taken as to the use of the data from half, double or any intermediate size specimens compared to the dimensions specified since there will be constraint effects on CCI and CCG. It is useful to obtain data from a benchmark standard size specimen for comparison with thinner/thicker or smaller/larger size testpieces.

8.3.5 *Specific size requirements*

No specific size requirements are imposed in this method. However, specimen size must also be chosen with consideration to the capacity of the loading and heating system, being able to fit the specimen into the heating furnace with sufficient room for attaching the necessary extensometers, and providing sufficient ligament size for growing the crack in a stable fashion to permit collection of crack growth data. For the case of the Laboratory specimens in Figure A.I.3: Generic edge cracked specimen defining B and B_n. Figure A.I.3 Section 4613.2 gives recommended dimensions which should be used if possible. Any variations in dimensions are allowed as long as the parameters are checked and verified.

8.3.6 *Specific side-grooving requirements*

For the case of the Laboratory specimens in Figure A.I.2 a generic edge cracked specimen defining B and B_n is shown in Figure A.I.3 (see Section 13.2). Side-grooving is required for these types of specimens. In general side-grooving of between 10-20% should be chosen in order to increase crack-tip constraint and direct the crack path at normal to the loading direction.

8.3.7 *Shape of the crack front*

Crack front straightness requires side-grooved specimens in most cases. The depth of required side grooves for a particular material might only be found by trial and error but a total reduction of 20 % has been found to work well for many materials. However, for extremely creep-ductile materials, a total side-groove reduction of up to 40% may be needed to produce straight crack fronts. Any included angle of side groove less than 90° is allowed. Root radius shall be $< 0.4 \pm 0.2$ mm. See Sections 8.3.10 for further information.

8.3.8 *Pre-cracking to introduce a sharp flat crack front*

There are two methods that are used for pre-cracking test specimens. The preferred method for deriving steady state CCG is to use an Electro Discharge Machine (EDM), especially for creep brittle conditions and also for 'Feature components', as it gives consistency and a sharp flat crack starter. Pre-cracking or a sharp crack starter should be carried out after the specimen has been side-grooved and cut to its final specification when EDM crack starter is used. The required cutting diameter should ideally not exceed a diameter of 0.2mm. The second method is to pre-fatigue the specimen. The details for this technique are given in ASTM E647 [g]. Historically pre-fatigue crack starters have been used in fracture toughness tests [f] and were adopted for CCG without a full consideration of its effectiveness and usefulness.

8.3.9 *Pre-cracking for CCI tests*

Where CCI data are affected by the initial crack-tip COD then the time to initiation might be substantially affected. If crack initiation 'CCI' is the primarily concern it is suggested that a comparison be made between fatigue crack initiation and EDM crack starters by testing two specimens. Pre-cracking or a sharp crack starter should be carried out after the specimen has been side-grooved and cut to its final specification when pre-fatigue crack starter is used. From previous experience it has been found that for long term tests and for creep ductile materials there is very little

effect due to the type of crack starter and for creep brittle materials EDM starter is essential since using pre-fatigue it is difficult to obtain the required crack tip length and linear shape.

8.3.10 *Crack length measurements*

For crack length measurements primarily a crack size monitoring equipment capable of reliably resolving crack extensions of at least ± 0.1 mm at the test temperature is recommended. The selected crack size measurement technique must be capable of measuring the average crack size across the thickness. Since crack extension across the thickness of the specimen is not always uniform, surface crack length measurements by optical means are not considered reliable as a primary method.

Optical observation may be used as an auxiliary measurement method. Where there is oxidation on the surface of the specimen the surface can be coated with a brittle high temperature paint which will adhere to the surface. This method is usually good where crack growth of > 5mm is measured. Usually the AC or the DC potential drop (PD) is used to measure increased resistance of the metal with crack extension [9]. However there are newer advanced techniques such as the laser measurement method [26] that can be used.

8.3.11 *The use of Potential Drop (PD)*

The use of potential drop (PD) technique is however the most commonly used method for crack size measurement during creep crack growth testing. DC or AC potential drop apparatus can be used and manufacturer's specifications should correspond with the stated accuracy for crack extension determination of ± 0.1mm as stated above. The data calibration for crack length is described in Sections 8.8.4 and 18.21.5. For the Feature Component tests in APPENDIX II there will be a need to monitor the crack along a longer crack front as in these specimens the crack front is not restricted by side-grooves. The best way to do this is to measure the PD in different regions and to compare the values with respect to the final crack shape.

8.3.12 *Preparing the specimens for PD leads*

Preparing the specimens prior testing consists of spot welding thermocouples and Potential Drop (PD) wires. For advice on positioning of the wires advice should be sought from the PD equipment manufacturer. Failing that it is suggested that the input wires should place remote from the crack tip (usually on top and bottom of the specimen and the output wires should be place on the opposite face of the specimen aligned near the crack tip. As long as the same relative positions are repeated from test to test acceptable signal repeatability will be obtained. The ideal condition is to achieve as high signal strength as possible. The linear interpolation method is proposed for estimating crack length and is described in Section 18.21.5. Optical observation may be used as an auxiliary measurement method. The selected crack size measurement technique must be capable of measuring the average crack size across the thickness.

8.3.13 *Specimen setup*

The specimens are set up in the loading rig using shackles designed specifically for the test rig with fittings compatible with the geometry to be tested. This means that regardless of the type specimen that is to be tested the machining precisions must be adhered to in order to reduce undue misalignment of loading. The test rig must be calibrated in accordance with the manufacturers' specifications. The test rig must in general be capable of achieving the test specifications outlined in this Section.

8.3.14 *Loading and creep displacement measurements*

Loading and creep displacement measurements for all the specimens in APPENDIX I need to be considered. Methods of measuring the Load-Line Displacement (LLD) or Crack Mouth Opening Displacement (CMOD) throughout the test essential for the calculation of C^* in Laboratory type

geometries (APPENDIX I) but not so for feature specimens identified in APPENDIX II. There are a number of methods that are available for making the displacement measurements. Direct capacitance gauge in the furnace is also available for long term tests. The measurements can also be made sensitive strain gauges from a point outside the furnace by measuring the CMOD by means of horizontal ceramic rods in contact with the side of the specimen or at the pin LLD by means of vertical metallic rods measuring separation at load-line. In all cases the accuracies to be achieved for measuring the displacement should be within ±1%.

8.3.15 *Displacement gauge*

The displacement gauge should ideally have a working range of no more than twice the displacement expected during the test. Accuracy of the gauge should be within ± 1 % of the full working range of the gauge. In calibration, the maximum deviation of the individual data points from the fit to the data shall not exceed ± 1 % of the working range. Knife edges are recommended for friction-free seating of the gauge. Parallel alignment of the knife edges must be maintained to within ± 1°.

8.3.16 *Heating of the specimens*

Heating of the specimens in the furnace to the relevant test temperature is by means of a suitable furnace. Test temperatures could range between 300-1200 ^{o}C depending on the material being tested. The criteria for heating should be that the temperature should be constantly monitored at various position of the specimen and that the temperature should not deviate from the range of ±1^{o}C. Usually a two or three zone furnace is used depending on the size of the specimen. The furnace controller should be such that it will be stable for long periods (up to or over a year) and the temperature controller is sufficiently sensitive that it will compensate the possible variations in the laboratory temperature.

8.3.17 *Initial pre-load*

An initial pre-load not exceeding 10% of the final load should be placed on the specimen. This assists in the alignment of the shackles and the specimen. The temperature should be kept at the test temperature for at least 12 hours in order that all the monitoring signals stabilize. The applied load is either held constant with time or at fixed displacement which has been pre determined using previous knowledge of the material behaviour and fracture mechanics methods to estimate the required lifetime. The load (or the displacement in the case of fixed displacement tests) is applied incrementally and slowly (over about 5 minute) ideally using a hydraulic loader.

8.3.18 *Monitoring the temperature*

Monitoring the temperature continuously will ensure that it will be maintained to within the allowable limits of ±1% during the test. The crack size, LLD and/or CMOD should be continuously recorded digitally, strip-chart recorders or both, as a function of time. If servo-mechanical loading systems are used to maintain constant load, or if tests are conducted under conditions other than constant load, a record of load versus time also must be maintained. It is suggested that for tests conducted under conditions other than dead-weight loading, the user should compare the results and verify the analysis to tests performed under dead-weight loading conditions.

8.3.19 *Unplanned temperature excursions*

Unplanned temperature excursions for any reason during the test must be logged. Any drop in temperature will not invalidate the test whereas increase in temperature of > 10^{o}C above the test period for >10% of the expected lifetime may invalidate a constant temperature test or part of the test depending on what information is sought.

8.3.20 *Initial pre-load*

An initial pre-load not exceeding 10% of the final load should be placed on the specimen. This assists in the alignment of the shackles and the specimen. The temperature should be kept at the test temperature for at least 12 hours in order that all the monitoring signals stabilize. The applied load is either held constant with time or at fixed displacement which has been pre determined using previous knowledge of the material behaviour and fracture mechanics methods to estimate the required lifetime. The load (or the displacement in the case of fixed displacement tests) is applied incrementally and slowly (over about 5 minute) ideally using a hydraulic loader.

8.3.21 *Specimen loading*

Specimen loading is by constant load for static creep tests and cyclic or dwell for creep/fatigue testing. However constant displacement or constant displacement rate tests are also relevant in CCI and CCG testing. In some cases where the material is very brittle (ε_f <10% uniaxial creep failure strain) or very stress sensitive with the creep index n >> 10 it is advisable to perform constant displacement tests rather than constant load tests. The accuracy of applied load of the testing machine shall be verified regularly to meet the requirement of ISO 7500-2 [jj].

8.4 Data Collection

8.4.1 *Detailed test and data monitoring*

Detailed test monitoring throughout the test is essential so that a clear history of temperature, PD and displacement is available. If servo-hydraulic machines are used under constant load conditions, the load must be monitored continuously and the variations in the indicated load must not exceed ± 1.0 % of the nominal value at any time during the test. If either constant displacement rate or constant displacement loading is used, the indicated displacement must be within 1% of the nominal value at any given time during the test.

8.4.2 *Data logging*

Data logging and taking additional readings at the beginning of the test when rapid changes occur is important. Also when the test nears its final stage and CCG begins to accelerate additional readings should be taken. A decision must be made at some point to stop the test when CCG begins to accelerate towards rupture. In this way any damage that might occur to the furnace will be avoided. It is ideal to stop the test just before failure or approximately when the specimen has reached 90-95% of life (see Section 8.4.3) for method of load displacement measurement during unloading in order to obtain the elastic compliance).

8.4.3 *Displacement measurements*

The displacement data should be logged all the way to full load starting from pre-load. This information is important both for the subsequent analysis of the data using C^*, K^c_{mat} (see Section 15) and validation (see Section 9.3.1). Note should be taken of possible instantaneous deviation from the elastic loading condition prior creep at or near zero time. This measure will give an indication of crack tip blunting and/or plasticity at full load (see Section 9). In addition the load/displacement measured will give the specimen's elastic compliance for the initial crack length. This information will be compared with the elastic unloading that will be similarly logged at the conclusion of the test prior final failure in order to quantify the extent of elastic to total creep displacement rate for the test. Section 9.3.3 will use this information to check for validity of analyzing the data using C^*. For this purpose the values of initial elastic displacement $\Delta^e_{e_i}$ at full load and the final elastic displacement $\Delta^e_{e_f}$ during the final unloading (before the test is broken in half) should therefore be measured and

logged in addition to the time increment t_{Δ} between the two readings and the corresponding total displacement at the initial and final time ($\Delta^{t}_{e_i}$ and $\Delta^{t}_{e_f}$). It is also possible to perform a load/unload operation once at sometime during the test if there was concern regarding a premature failure of the testpiece. This information is used in Section 9.3.2 as a check for test and parameter validity.

8.5 Post-Test Measurements

Post-test measurements should be carried out on the specimen. Any dimensional changes, necking, crack front shape and observing the fractured surface should be recorded in detail. Detailed metallography to observe damage ahead of the crack tip, especially when crack initiation is of interest should be performed. In order to look at crack tip damage development on completion of the test, half of the specimen, normal to the crack plane, is cut using EDM and the other half is broken. In this way one half of the specimen section can be polished and observed using metallography. In some cases for tests involving weld, HAZ or cross-weld specimens it is also useful to make micro-measurement hardness in the region of the crack tip, if the equipment is available.

8.5.1 *Measurement of the final crack front*

An accurate measure of the final crack front and crack size should be made when the specimen is finally breaks or is broken open outside the furnace. Section The total crack extension, Δa_f, is derived by subtracting the initial crack size, a_i, from the value of the final crack size, a_f. The final crack size shall be determined from surface fractography measurements where possible. The initial and final measured crack length is used to compute incremental crack length in Sections 8.8.4-18.21.5 using PD measurements obtained during the test.

8.5.2 *Crack tip bowing*

Crack tip bowing, if any, at the final crack length a_f, should be measured in detail using optical methods. There could be a possibility of crack tip bowing with either the centre or the surface of the specimen showing faster crack advance. This will depend on the stress state. Once the specimen has been cut (see Section 0) the crack size is measured on half of the specimen at four equally spaced points centered on the specimen mid-thickness line and extending to $0.005W$ from the roots of the side-groove. The crack size used is the average between the center and the surface crack lengths. If the ratio due to crack tip bowing between the crack tip centre and the surface is >20% the longer final crack length a_f should be recorded. The use of the longer crack length in the analysis will invariably give a more accurate estimate for CCG predictions. Consideration should also be given to increase or decrease side-grooving in a subsequent test in order to obtain a straight fronted crack. The measuring instrument shall have an accuracy of 0.025 mm. If there is failure to stop the test before making the measurements the observations should make use of oxide surface markings using fractography to identify the crack tip profile.

8.5.3 *Crack extension criteria*

The crack extension of 0.5 mm is adopted as the 'engineering' limit for CCI. Thus if crack extension $\Delta a \leq 0.5$ mm then time to CCI can be estimated and correlated in accordance with the method shown in Section 11.2. When $\Delta a_f > 0.5$ mm, then both time to CCI and CCG rate behaviour (as described in 11.1 and 11.2) should be carried out. In both cases the test for steady state creep condition, as shown in Section 9.3.1, should be performed and the times logged accordingly.

8.5.4 *Crack deviation criteria*

If the crack deviation during the test is outside an envelope that encompasses the material between the planes that are oriented at ± 5° from the idealized plane of crack growth and that intersect the axis of loading, the data are invalid by this test method. However the data should be logged. It is then

possible by extending and/or changing size of side-grooving and geometry to alleviate this problem in subsequent tests.

8.6 Recommended Minimum Number and Duration for Tests

Material property values are interpreted as constants which can be used to help characterize the material in processing and design. Since material 'basis' values will always vary from one set of data to the next, even if the material, conditioning, and test remain unchanged, treating them as material constants is always an approximation. However, if the calculations are based on 'enough' data, the basis values should be reproducible, to within engineering accuracy, across comparable data sets. The objective of this document is to highlight problems associated by the small-sample reproducibility and to provide guidance on how many data are necessary in basis value calculations in order for these values to be approximately reproducible. How many data are 'enough' depends on many factors, including

1. The statistical model which is used to approximate the population, from which the data is sampled,
2. Accounting for the anisotropy of the material,
3. The degree of reproducibility which is desired,
4. The variability in the property being measured,
5. Variability in measurements of the property due to the test method,
6. Accuracy of the equipment,
7. Cost and the capability of performing numerous tests.

Because of these factors, it is impossible to give firm recommendations. Batch to batch variation is more important in welds and cross-welds samples than in parent metallic materials. This is due to sensitivity of the properties on fabrication processes. Background information and guidelines about fabrication and test-piece preparation to assist the tester in making a sample size decision should be planned. It should be emphasized that differences and the stability of the material basis values with respect to sample size and geometry needs to be taken into account. The recommendations arrived at based on previous experience and available statistical analyses [64-69].

8.6.1 *Batch to batch variability*

It is important to recognize that for the purposes of design or remaining life assessment, inherent material variability often becomes the primary source of scatter in CCG rate (*da/dt)*. The variability associated with a material is caused by inhomogeneity in chemical compositions, microstructure, or both. These same factors coupled with varying processing conditions give rise to further batch to batch variability. An assessment of inherent material variability, either within or between heats or lots, can be determined only by conducting a statistically planned test program on the material of interest. This may involve substantial number of tests.

8.6.2 *Minimum test requirements*

The requirements given in this Section are made for laboratory tests and not feature component tests as it is unusual that material basis properties are derived from such tests. It should be noted that the main objective of the exercise in to derive the mean line of the data at the first instance. This will need less number of tests. The true upper-lower bounds of a dataset would usually need substantial numbers of tests and it is usual to perform limited numbers of tests and to subsequently perform a simple statistical analysis to derive the standard deviations from the mean. There are two kinds of data sets that need to be considered. The first is a single point data derived from a single test such as creep uniaxial rupture tests and CCI test and the second are the tests that produce numerous data points such as the creep strain rate in a uniaxial test and FCG or CCG rate tests.

8.6.3 *Single point data per test*

The decision regarding the minimum numbers for single point tests are dependent on the quality of the derived mean value using the least squares best fit. The data points should ideally spread evenly within the required range or duration of data (ideally in creep tests they should spread evenly over 2 or more orders of magnitude of time). For an ideal condition a minimum of 10 tests per batch and condition is recommended [64-69]. However it is important to note for new materials or welded specimens, where there is no prior knowledge of the specimens' behaviour, with respect to the load conditions and their sensitivity to the stress or strain range, the failure times or number of cycles to failure, the minimum number of tests that should be performed would need to be greater than 10. To be conservative, for new material and welds and cross/welds at the same testing condition, as many tests as 20 and some with repeat loading, evenly spread over the required stress range, should be planned in order to reduce the errors in the distribution of the data.

8.6.4 *Multiple points data per test*

For multiple data point tests, to derive the mean line, it is suggested that a minimum of five tests, each with a minimum of 10 data points, at different loads should be performed for FCG and CCG rate tests. These should overlap and cover at least two decades of crack growth in duration. If the materials exhibit such factors as irregular voids, large grains, weld, X-weld, HAZ and other non-homogeneities the minimum number of tests should be increased to 10 in order to obtain the optimized values for the mean and the standard deviation of the data. Also more tests should be performed if the material CCG behaviour exhibits increased scatter regardless of the reason for the variability. If there is insufficient availability of the material or if there are other reasons which would restrict multiple testing then the results should be considered with increased caution.

8.6.5 *Test duration requirements*

A note regarding the duration of test times is appropriate at this point. Due to the time-dependent nature of creep and its non-linear behaviour it is essential to obtain data that can be described as 'long-term'. In practical terms this could mean test times ranging from 1000 to 10,000 which are still lower when compared to most component design lives. It is obviously preferable that as long a test time as possible should be achieved in order to obtain stress state conditions and material properties which are closest to the long term component data. This is not always possible, and should therefore not be an essential objective, since predictive CCI and CCG models and life assessment methods should be used to take this difference into account. However in order to apply the predictive fracture mechanics models correctly it should be ensured that the CCI and CCG test time range and references stress levels are in same range as the uniaxial material properties data that is to be used in the modeling process.

8.7 Sensitivity and Accuracy Limits of the Results

It is vital that due care attention is placed on the test and measurement techniques in order that the limits of accuracy are maximised. Due to the stress sensitivity in creep any error in testing is magnified in the analysis. This can be dealt with using upper/lower bound or statistical methods to analyse the data.

8.7.1 *Effects of data variability on correlation for FCG, CCG and CCI*

The correlation of *da/dt* versus *C**, or *K* or any other parameter is a function of inherent material properties, variability as well as errors in measuring crack size, temperature, creep displacement rates and applied load levels. The required precisions stated in Section 4.4 are readily attained by modern creep machine equipment and by servo-mechanical test machines. However any deviations and scatter beyond the stated accuracies should be dealt with statistically.

For example, based on average creep properties, a ± 1 % variation in load can lead to about ± 4 to 12 % variation in the value of C^* and 1% variation in K. This translates to ± 3 to ± 10 % variation in da/dt, at a given C^*. However, in general the crack size and displacement measurement errors cause a more significant contribution to the variability in da/dt although this contribution is difficult to isolate since it is coupled to the analytic procedure for converting a versus t and Δ versus t to da/dt and $d\Delta/dt$, and to the inherent variability in the material. Nevertheless, it is clear that the overall variation in da/dt is dependent on the ratio of crack size and displacement measurement interval to measurement error. Furthermore, an optimum crack size measurement interval exists because of the fact that the interval should be large compared to the measurement error (or precision), but small in comparison to the C^* gradient of the test specimens. These considerations form the basis for the recommended intervals for data reduction.

8.8 Preparation of Test Data

The test information collected during a long term creep test will invariably be substantial and detailed. In some cases the logged data which will be at short time increments could exceed thousand of points and will usually contain a degree of noise. The steps taken to perform the data reduction are as follows.

8.8.1 *Data collection*

The data that are collected in increments of time and will consist of the potential drop for crack length estimation, the load-line displacement or the load in the case of fixed displacement tests. The temperature details are also logged for checking purposes. The rate of collecting this data should be higher for the early and the final stages of the tests as variations of the data during these periods are rapid.

8.8.2 *Time at which the test should be stopped*

The test should be stopped as soon as both the potential drop and the displacement measurement indicate that the tertiary stage of crack growth has begun and that final failure of the specimen is imminent. In this way the necessary unloading measurements can also be taken (see Section 8.3.15). The crack extension can be determined from the electric potential reading using the linear interpolation method as shown in 8.8.4.

8.8.3 *Smoothing the PD output data*

It is recommended that the value of PD be extrapolated back to zero time from where the signal is stable and increasing in a steady manner. This smoothing operation can usually be performed from a position of about $0.5\Delta V_f$ on the PD versus time plot (where it is clear that the PD response is primarily due to crack growth). This operation could lead to an adjustment of the initial PD value V_i. From this operation the initial and final PD values are identified. This information is used in Section 18.21.5 to estimate the crack extension increments.

8.8.4 *Deriving the crack length from the PD output*

The crack length is usually derived from the PD output. The initial and final PD values (Vi and V_f) need to be determined to estimate crack length using Section 18.21.5. Usually the PD signal is stable and consistent. However there are occasions where anomalies or intermittent signal loss or jump may occur for which the cause must be sought. Also in the early stage of the test (usually the first few hours any change in the PD response would be due to loading, and initial crack tip blunting that may occur). It should be noted that in some cases the initial PD readings at the beginning of the tests could drop before stabilization and eventually increase with crack extension. Conditions of initial loading, plasticity, excessive creep and damage and crack tip oxidation could affect the extent of this drop in the PD. Therefore there is a likelihood of increasing scatter in crack size measurements

during the initial periods of testing. Judgment may be needed in preparing the PD data. Sections 18.21.5 and 18.21.6 in APPENDIX V describe the method for calculating crack length from the available PD output.

8.8.5 *Recommended number of data points*

Once the incremental crack length and displacement values have been derived the number of data points over the test time should realistically be reduced to a workable level of 20-40 whilst at the same time making sure that no relevant information is lost. This is especially important at the early stages of the test. This can be done either by smoothing the data by eye or using the various available data fit software. In both methods care and judgment should be exercised to make sure that the fit is representative of the actual data and anomalies scatter are individually checked and either left as data or deleted. Valid reasons for the deletions should be given. In cases of creep/fatigue loading the analysis is performed at the maximum load readings. However the upper/load levels, R-Ratio, load cycle shape and frequency should all be recorded.

8.8.6 *Calculating cracking and displacement rates*

da/dt and $d\Delta/dt$, which have been checked for validity in Section 9, are derived from the smoothed data using the seven-point reduction technique specified in Section 18.21.3. The data for the initial and final periods of the test should be at shorter increments as these regions show larger variations. Subsequent analysis for CCI and CCG can be carried out as specified in Sections 9 and 11.

9 DATA ANALYSIS PROCEDURES

Expressing *da/dt* as a function of an appropriate crack growth rate correlating parameter generally provides results that are independent of specimen size and planar geometry for the same stress state at the crack tip. Thus, the appropriate correlation will enable exchange and comparison of data obtained from a variety of specimen configurations and loading conditions. Moreover, this feature enables creep crack growth rate data to be treated as a material property and to be utilized in the design and evaluation of engineering structures operated at elevated temperatures where creep deformation is a concern.

9.1 Choosing an appropriate CCI or CCG rate Correlating Parameter

9.1.1 *Choice of parameter for correlating CCG*

The collected and reduced data is correlated versus relevant fracture mechanics parameters. The details of the parameters and their derivations are given in (12). The choice of the most appropriate crack growth rate relating parameter depends mainly on whether the material exhibits creep-ductile or creep-brittle behavior9.3). In this procedure emphasis is place on the use of the C^*, K or ΔK (only Fatigue) parameters as they are the most validated parameters in use.

Fracture mechanics parameters K and C^* are by far the most prevalent method that are employed for the analysis of the data [27]. More recently parameters such as K^c_{mat} [see APPENDIX II :(TDFAD)], [61] the Q^* [APPENDIX III: The Q*] [49-53] and the Local Crack–tip Displacement (CTOD) approach [see APPENDIX IV: Local CTOD Approach] [42,43] have been proposed which may be appropriate for analyzing crack initiation and growth data. Outline of these methods are presented in appendices II, III, IV (Sections 15,16,17).

9.1.2 *Choice of the C* term for CCG rate*

Steady-state creep crack growth rates in creep-ductile materials, exhibiting extensive creep, are correlated by $C^*(t)$ which degenerated to the steady state C^* (as identified throughout this document). In the small scale creep region the parameter C_t [3,7,10] could also be used. However it

has been found that for most practical situations in laboratory test-pieces, it can be assumed for the range of crack lengths observed, that $C^*(t) \cong C_t$ (see Sections 9.2.6-9.3.5). Given also the fact that the differences between C_t and $C^*(t)$ are at worst below a factor of two (see Sections 9.2.6-9.3.5). it can be seen that within the overall scatter spread of CCG data observed [64-69] the detailed analysis in a multi-point test (see Section 8.6) using either method will not affect the overall trends in the data. In fact when analyzing CCI data which uses only one point per test ((see Section 8.6)) there is even more scatter [64-69] making the effect of choice of C^* choice insignificant. Therefore this procedure, in order to unify the output of results from different laboratories, will adopt the steady state C^* for use in the correlation of the data in the valid region described in Section 9.3.

Note 2: At high loads the time to redistribution is further reduced due to plasticity. Therefore for most practical circumstances it is found that the steady state C^* adequately describes the stress distribution ahead of a growing crack for most of the testing period.

9.1.3 *Choice of parameter for CCI*

Initiation of the crack (CCI) could constitute a major portion of the time to failure. Detailed estimation of the early stages of cracking rate, especially the 'tail' section, remains to be clarified as the shape and period of the tail needs further clarification [9,70]. By using K or C^* to correlate the time to a specific crack extension following loading this problem can be circumvented to a good extent. Therefore the data for initiation times to a crack extension of 0.5 mm (described as the 'engineering "initiation" limit' for CCI) can be correlated versus K or C^*. In most cases initiation times are inversely proportional to the parameters. Same condition regarding the validity of K or C^* will apply as specified for CCG.

9.2 Definitions for the relevant Fracture Mechanics Parameters

9.2.1 *Stress intensity factor, K*

Stress intensity factor, K is the magnitude of the ideal crack tip stress field (a stress-field singularity) for Mode 1 in a homogeneous, linear-elastic body. There are extensive description and analysis for K found in the literature [55-59]. K is a function of applied force and test specimen size, geometry, and crack length, and has the dimensions of force times length$^{-3/2}$ tabulated in APPENDIX I are the K formulae for the specimens described in Section 13.2.

9.2.2 *J-integral*

J-integral is a mathematical expression of a line or surface integral that encloses the crack front from one crack surface to the other it is used to characterize the local stress-strain field around the crack front. The J-integral concept is related to creep analogously relating deformation in plasticity to creep deformation assuming the stress distribution at the crack tip remains the same by going either route. Therefore for a work hardening material and a creeping material following Norton's creep law the stress-strain field, due to plasticity) is identical to the stress-strain rate field due to creep. There are available in the literature [59] numerical expression of J for the geometries shown in Section 13.2.

9.2.3 *The C* parameter*

The C^* integral has been widely accepted and used as a parameter for correlating CCG and CFCG under steady state creep conditions [1-11]. The theory behind the correlation of high temperature crack growth data essentially follows those of elastic-plastic fracture mechanics theory. Various aspects of the characterization of creep crack growth have been reviewed and this document only give an outline of the C^* derivation and its link to plasticity.

The parameter relevant to creep crack growth is given as the $C^*(t)$-Integral consisting of a line or surface integral that encloses the crack front from one crack surface to the other. $C^*(t)$ is used to

characterize the local stress-strain rate fields at any instant around the crack front in a body subjected to extensive creep conditions. The $C^*(t)$ expression for a two-dimensional crack, in the x-z plane with the crack front parallel to the z-axis, is the line integral:

$$C^*(t) = \int_{\Gamma} \left(W^*(t)dy - T.\frac{\partial \dot{u}}{\partial x} ds \right) \tag{1}$$

where:
$W^*(t)$ = instantaneous stress-power or energy rate per unit volume,
Γ = path of the integral, that encloses (that is, contains) the crack tip,
ds = increment in the contour path,
T = outward traction vector on ds,
$\dot{u}$ = displacement rate vector at ds,
x, y, z = rectangular coordinate system and

$$T.\frac{\partial \dot{u}}{\partial x} \partial s \tag{2}$$

is the rate of stress-power input into the area enclosed by Γ across the elemental length ds. The value of $C^*(t)$ from this equation is path-independent for materials that deform according to the following constitutive law that is separable into single-value time and stress functions of the form:

$$\dot{\varepsilon} = f_1(t) f_2(\sigma) \tag{3}$$

where f_1 and f_2 represent functions of elapsed time, t, and applied stress, σ, respectively; $\dot{\varepsilon}$ is the strain rate. For materials exhibiting creep deformation for which the above equation is path-independent, the $C^*(t)$-integral is equal to the value obtained from two, stressed, identical bodies with infinitesimally differing crack areas. This value is the difference in the stress-power per unit difference in crack area at a fixed value of time and displacement rate, or at a fixed value of time and applied load. The value of $C^*(t)$ corresponding to the steady-state conditions is called C^*. Steady-state is said to have been achieved when a fully developed creep stress distribution has been produced around the crack tip.

9.2.4 *Creep zone*

Creep zone boundary-the creep zone boundary is defined as the locus of points ahead of the crack front where the equivalent strain caused by the creep deformation equals 0.002 (0.2%).Under small-scale creep conditions, the creep zone expansion with time occurs in a self-similar manner thus, the creep zone size, r_c [6-8], can be defined as the distance to the creep zone boundary from the crack tip at a fixed angle θ with respect to the crack plane.

9.2.5 *Steady state creep*

Under steady state creep conditions, the crack tip stress and strain rate fields are characterized by the parameter C^* and linear elasticity may no longer be applicable [28]. For a power law creeping material, the stress and strain rate in the vicinity of the crack tip are given by,

$$\sigma_{ij} = \sigma_0 \left(\frac{C^*}{\dot{\varepsilon}_0 \sigma_0 I_n r} \right)^{1/(n+1)} \tilde{\sigma}_{ij}(\theta, n) \tag{4}$$

$$\dot{\varepsilon}_{ij} = \dot{\varepsilon}_0 \left(\frac{C^*}{\dot{\varepsilon}_0 \sigma_0 I_n r} \right)^{n/(n+1)} \tilde{\varepsilon}_{ij}(\theta, n) \qquad (5)$$

where r and θ measure distance and polar angle relative to the crack tip respectively, I_n is a parameter which depends only on the creep exponent, n, and $\tilde{\sigma}_{ij}$ and $\tilde{\varepsilon}_{ij}$ are dimensionless functions.

9.2.6 *The C_t parameter*

Parameter, C_t, is a parameter equal to the value obtained from two identical bodies with infinitesimally differing crack areas [3,7,10], each subject to stress, as the difference in the stress-power per unit difference in crack area at a fixed value of time and displacement rate, or a fixed value of time and applied load for an arbitrary constitutive law. The value of C_t is path-independent and is identical to $C^*(t)$ for extensive creep conditions (see Section 12) and further differs by more than a factor of 2 for the wide range of C^* applicability.

9.2.7 *Small-scale creep*

Under small-scale creep conditions, $C^*(t)$ is not path-independent and is related to the crack tip stress and strain fields only for paths local to the crack tip and well within the creep zone boundary. Under these circumstances, C_t is related uniquely to the rate of expansion of the creep zone size. There is considerable experimental evidence that the C_t parameter which extends the $C^*(t)$-integral concept into the small-scale creep and the transition creep regimes and is equal to $C^*(t)$ in the extensive creep regime, correlates uniquely with creep crack growth rate in the entire regime ranging from small-scale to extensive creep regime. In addition it has been shown in a VAMAS special edition [11] that K can also correlate CCG where creep brittle conditions dominate.

9.2.8 *Interpretation of C^* parameter*

In most cases under steady conditions the parameter C^* is used (see Section 9). It may be obtained numerically from a path independent integral and is analogous to the J integral for rate independent material behaviour. However for the purposes of this CoP the C^* parameter will be interpreted as an energy release rate analogous to the energy definition of J and by using the reference stress method (see Sections 16.5.2, 14.3,14.5.2).

$$C^* = -\frac{1}{B}\frac{dU^*}{da} \qquad (6)$$

where a is the crack length, B is the thickness and U^* is the potential energy rate. This form can be used in the laboratory tests, rather than use the line integral definition or Equations ((4)-(5)). In addition a reference stress creep strain rate interpretation method can also be used to derive C^*. The experimental and the reference stress methods are put forward in this CoP (see Section 12.) as the proposed method for deriving C^*. However validated numerical methods for the derivation can also be used.

9.2.9 *Time Dependant Failure Assessment Diagram (TDFAD) for CCI*

The TDFAD is based on the Option 2 FAD (failure assessment diagram) specified in R6 [31] which involves a failure assessment curve relating the two parameters K_r and L_r, and a cut-off L_r^{max}. The derivation of a creep toughness parameter K^c_{mat} is taken for the simplest case of a single primary load acting alone [60-62]. The details of definition of K^c_{mat} are as explained in Section 15. The method is appropriate for analyzing CCI data.

Note 3: TDFAD method for crack initiation has been incorporated into R5 [30]. However it has not been fully validated for all the geometries in this CoP.

9.2.10 *The Q* Parameter*

Q^* which is a thermal activation based parameter describes creep-ductile and creep-brittle [49,51] steady state region of creep cracking rate using the general expression $da/dt = A\ exp(Q^*)$. Q^* is a non-dimensional function of applied force, test specimen size, geometry, crack length, activated energy, gas constant and testing temperature and is proportional to the local elastic or the elastic-plastic field depending on its mode of use. The details of definition of Q^* are as explained in Section 16. It has been validated for cracked notched specimens.

Note 4: The Q^* method has not been validated in the present version of this CoP.

9.3 Criteria for Validity Checks of *C* and K*

Once the calculations of the parameters are completed in accordance with the guidelines in Section **12** validity checks should be performed which are outlined in this Section.

9.3.1 *Check for validity of C**

These conditions establish to what extent K or C^* parameters are valid at the crack tip. They are by no means rigorous as there are a number of unknowns in play such as the variability in estimating actual plasticity, variability and changes in creep properties (used in deriving t_T) due to stress and cracking rates. Given these factors all data should be examined regardless of these criteria and subsequent judgment should be made to identify the important trends such as the steady state CCG region and the times taken to CCI.

A check for validity of the steady state C^* parameter consists of a number of conditions being fulfilled. The details are set out in the following three Sections. The criteria are as follows.

[a] Upon initial loading specimen does not undergo extensive plasticity (this can be determined by making sure that the initial crack-tip deformation measured at LLD, Δ^{LLD} or CMOD, Δ^{CMOD} would be <0.05 W).

[b] During the test the specimen does not undergo extensive creep (this can be determined by making sure that the total deformation during the test measured at LLD or CMOD is <0.05 W).

[c] The ratio of creep displacement rate/total displacement rate $\dot{\Delta}^c / \dot{\Delta}^t \geq 0.5$ or $\Delta^c_{(e_f - e_i)} / (\Delta^t_{e_f} - \Delta^t_{e_i}) \geq 0.5$. (see Section 12.1).

[d] Experimental test times $t >> t_T$ to make sure that steady state C^* is valid. (see Section 9.3.5)

9.3.2 *Components of displacement rates*

Throughout the test the total displacement rate $\dot{\Delta}^t$ is measured. Section 12.1 identifies the creep, elastic and plastic components of the displacement and suggests the appropriate values that should be used in the C^* analyses. Generally it can be said that the criteria for the applicability of C^* are put in place to ensure that extensive creep, or plasticity or elasticity ratios which reduce the applicability of C^* in the analysis are identified.

Therefore by disregarding plasticity (except where it is extensive at high loads (see Section 18.20) then creep and elastic displacement rates ($\dot{\Delta}^c$ and $\dot{\Delta}^e$) can just considered hardly affecting the value of C^* calculated. There are available numerical estimates of Δ^e (at LLD or CMOD positions) [i]. For the geometries listed in Section 13 using elastic stress intensity factor Equations **(A.I.29)(A.I.29** to **(A.I.42**) (see APPENDIX I38) it is possible to derive the elastic component for the displacement. The allowable condition for applying C^* steady state to apply in this case is that $\dot{\Delta}^e / \dot{\Delta}^t \geq 0.5$ should be met throughout the test. This can be tested by incrementally checking $\dot{\Delta}^c$ and calculating the $\dot{\Delta}^e$ component from either the compliance of the specimen or numerical calculation of $\dot{\Delta}^e$ and plotting $\dot{\Delta}^c / \dot{\Delta}^t$ versus test time. Alternatively an experimental check (if the measuring equipment is sufficiently accurate) over a length of crack extension or time increment can be made by using the unloading measurement suggested in Section 8.4.3 and checking to see if the incremental ration of creep displacement given by

$$\Delta^c_{(e_f - e_i)} = (\Delta^t_{e_f} - \Delta^t_{e_i}) - (\Delta^e_{e_f} - \Delta^e_{e_i}) \tag{7}$$

Gives

$$\Delta^c_{(e_f - e_i)} / (\Delta^t_{e_f} - \Delta^t_{e_i}) \geq 0.5 \tag{8}$$

or as derived incrementally

$$\dot{\Delta}^c / \dot{\Delta}^t \geq 0.5 \tag{9}$$

Once either criteria are met the right condition is established for steady state C^* estimation. Subsequently using the formulae in Sections 14.3-14.5 C^* for the data analysis can be determined using the total measured displacement rate $\dot{\Delta}^t$.

9.3.3 *Validity criteria for C* for highly ductile materials*

When working with highly ductile materials it is important to determine the extent of plasticity at initial loading and also creep during the test. With reduced constraint and increased creep ductility C^* is unlikely to give a good description of the crack tip stresses. The extent of plastic deformation can be estimated using available plasticity calculation to estimate the deflections (see Section 18.20). However this is difficult as the analysis is extremely sensitive to the tensile properties data that is used. More conveniently if data acquired upon loading shows that the initial LLD or CMOD exceeds $0.05W$, which would be due mainly to plasticity, then the analysis using C^* is considered invalid (see Section 9.3.4). This usually occurs at high load or very ductile conditions due to plastic properties at the relevant temperature.

Note 5: Extensive creep during the test giving CMOD or LLD measurements in excess of $0.05W$ would render the C^* analysis to correlate CCG rate as void.

In both cases increased deformation suggests that stable CCG would not be achievable with the combination of material, geometry, size and temperature chosen. The most probable method of failure would be failure by rupture in these instances. The suggestion would be either in increase specimen size and/or side-grooving or choose a highly constrained geometry or reduce test temperature to overcome the problem.

Note 6: For creep ductile situation the parameter K^c_{mat} (see Section 15) could also be used in correlating CCI data. However these are not fully validated in the present version of the CoP.

9.3.4 *Validity criteria for creep brittle materials*

In creep-brittle materials (usually with uniaxial failure strain ε_f <10%) which constitute a small portion of the observed component creep behaviour, C^* might not be valid. When $\dot{\Delta}^c / \dot{\Delta}^t \leq 0.25$ or $\Delta^c/(\Delta^t_{ef} - \Delta^t_{ei}) \leq 0.25$ for which the data are classified as being creep-brittle the candidate parameter is K rather than C^*.

Note 7: For creep-brittle situations parameters K^c_{mat} (see Section 15) and Q* (see Section 16) might also be used in correlating the data. However these are not validated in the present version of the CoP and further advice should be sought.

9.3.5 *Transition time criteria for C**

The final condition to allow the application of C^* is that it must be established that test times are greater than the transition time, $t >> t_T$, beyond which point it is assumed $C^* = C^*(t) \approx C_t$. To determine the transition time t_T the following estimation is employed;

$$t_T = \frac{K^2(1-\nu^2)}{E(n+1)C^*(t_T)} \qquad (10)$$

The calculation of t_T varies with the value of $C^*(t_T)$. For each test time increment starting from zero the instantaneous transition time t'_T is calculated and plotted versus $C^*(t_T)$. The transition time t_T *is* then the first peak value of t'_T in the data set. Data for which time exceeds the transition time, t_T, are correlated by C^* as calculated in Section 14.3.

Also expression $\boldsymbol{C_t}$ which exists [10] for small scale creep analysis can be approximated to $C^*(t)$ as

$$C_t = \left[1 + \left(\frac{t_T}{t}\right)^{\frac{n-3}{n-1}}\right] C^*(t) \qquad (11)$$

This relationship suggests that for most circumstances the values of $C^*(t)$ is at most lower by a factor of 2 compared with C_t which can occur when $t_T \approx t$ (see also Sections 9.1.2-9.2.6).

Note 8: The data for which time is $t \leq t_T$ are correlated only by $C^*(t)$, C_t or K^c_{mat}. However these are not fully validated in the present version of the CoP.

Note 9: If there is found to be some extent of plasticity upon loading of the specimen it can be assumed that t_T estimated from the above equation will be conservative as plasticity itself will assist in the relaxation at the crack tip. However extensive plasticity in itself will deform the specimen and render the CCG as invalid (see above Section9.3.3).

Note 10: The analysis of data and the two methods of estimating C^* are shown in Section 12.

10 REPORTING PROCEDURES

10.1 Details of test information to be reported

Generally since creep tests last for long periods substantial amount of information is logged. In order to have available all relevant data it is sometimes necessary to keep information which may at the time not be regarded important or misleading. Therefore the requirements are that all data should be kept and recorded regardless. Data reduction can then be carried out and used subsequently for analysis. Detailed below is the type information that needs to be logged.

10.1.1 *Report of findings*

The users are advised, in any event, to correlate FCG, CCI and CCG data with K and C^* using the formulae given in Section 14.5.2 and report their findings without deleting any data. The plotting of the data using both methods would also act as a guide as to which methods will correlate the data better and how the cut-off criteria described for CCG in Section 11 would affect the trends in the data.

10.1.2 *Pedigree of the material*

Pedigree of the material, material composition, heat treatment, history, blocks size orientations, type of manufacture (for example, sheet, plate, and forging) and position of specimen extraction. Detailed dimensions of the specimen after machining should also be recorded to compare with the nominal dimensions. All information should be labeled and specimens numbered.

10.1.3 *Material properties to be logged*

All available material properties both at room and at testing temperature should be reported. For example tensile properties such as the Young's modulus, yield strength, failure strain, creep index, stress rupture index, creep failure strain should be available. If this is not possible generic material data could be substituted when defect assessment analysis requires this data.

10.1.4 *Test machine description*

Description of the test machine and equipment used to measure, temperature crack size and LLD or CMOD should be available. The precision with which measurements were made should be specified.

10.1.5 *Details of starter crack*

Details of pre-cracking or starter notch performed such as EDM or pre-fatigue. If fatigue pre-cracking was performed then the terminal value of K, P_{max}, P_{min}, the pre-cracking temperature, and the frequency of loading and the number of cycles used for fatigue pre-cracking. If pre-crack loads were stepped-down, state the procedure employed for the loading method and give the amount of crack extension at the final load level. If an EDM notch is used in-lieu of a fatigue pre-crack, report the root radius and the length of the notch. The size of the pre-crack extension from the machined notch should be no less than 5% of the totals crack size and not less than 1.3 mm. Care must be exercised during pre-cracking by either method to avoid excessive damage at the notch rule.

10.1.6 *Details for loading*

Details of loading, static or cyclic, and experimental variables such as room temperature and test environment should be specified. For environments other than laboratory air, report the chemical composition of the gas should be specified.

10.1.7 *Report of data analysis*

Report data analysis methods, including the technique used reduce data and to convert crack size and deflection data into rates and the specific procedure used to correct for discrepancies between measured crack extensions on the fracture surface with that predicted from the electric potential method.

10.1.8 *Plots of data*

Plots of corrected crack length versus time, total displacement versus time should be made available. After analysis plot of *CCG rate (da/dt)*, versus *C* or K* and for FCG rate (*da/dN*) versus ΔK should be made using log/log axes. It is recommended that *C* or K* be the abscissa and the cracking rate, be the ordinate. Estimated times to CCI versus *C*, K* or K^{c}_{mat} should also be plotted using log/log axes.

10.1.9 *Tabulation of results*

It is desirable to tabulate test results when using this test method for presentation of results. In addition to recording the load, temperature, the following information should also be tabulated for each test: a, t, Δ, da/dt, $d\Delta/dt$, C^*, K, t_T. σ_{ref}, time taken to reach Δa=0.5mm. The values of initial crack length a_i and elastic loading displacement Δ_i and the final crack length a_f and the final elastic loading displacement Δ_f should also be tabulated for checks to be performed in Section 9. All data that violate the validity criteria should be reported and identified in appropriate tables and plots.

10.1.10 *Photographic/micrographic evidence*

It is useful to have photographic/micrographic evidence for the different stages of the test. For example it would be useful, but not strictly necessary to have details on features showing the laboratory set-up, the untested specimen, the failed specimen, the surface feature, the mode of failure (intergranular for creep), and any special surface markings on the fracture surface due to damage, cracks or temperature.

10.1.11 *Treatment of anomalous data*

Description of any occurrences that appear to be related to anomalous data (for example, transient behavior following test interruptions or changes in load-levels, temperature or possible errors in equipment should be made available. The facts surrounding the event and possible reasons for them should be stated.

11 CORRELATING CRACK GROWTH USING FRACTURE MECHANICS

Crack growth in creep (CCG) can be described in various ways using different correlating parameters. However two parameters; the stress intensity factor, *K* and *C** have been widely used [1-27], both in test data and in life assessment codes to correlate CCI and CCG data at elevated temperatures. In fatigue cracking FCG the stress intensity factor is used to correlate crack growth per cycle as a function of the ΔK. The region of interaction for creep and fatigue is known to be limited and it has been found, where cyclic loading occurs at high temperatures [20,30,34] that a simple linear summation rule is sufficient to add the two components. A short description of the choice for appropriate parameters is given below the following Sections.

11.1 CCG rate analysis

Crack growth in creep and fatigue can be described in various way using different correlating parameters. However parameters such as the stress intensity factor, *K* and *C** have been widely used, both in test data and the codes to correlate creep crack growth rate data at elevated temperatures. The correlations of steady state crack growth rate with *K*, reference stress and *C** can be represented by straight lines of different slopes on log/log plots and expressed by power laws of the form

$$\dot{a} = AK^{m} \tag{12}$$

$$\dot{a} = D_o C^{*\varphi} \tag{13}$$

where A, D_o, m and φ and are material constants. A steady state relationship between crack growth rate and the parameters in Equations (12),(13),(14) and, physically imply a progressively accelerating creep crack growth rate. The elastic stress intensity factor K and the C^* parameter have generally been proposed for creep-brittle and creep-ductile materials, respectively. However it is necessary to verify the suitability of any of these parameters with respect to crack growth prediction in different materials.

The choice of the most appropriate crack growth rate relating parameter depends on whether the material exhibits creep-ductile or creep-brittle behaviour. Validity Criteria will be described in Section 9.3.1.

11.2 Crack Initiation (CCI) Analysis

When a structure containing a defect is first loaded the stress distribution is given by the elastic K-field or the elastic-plastic J-field. Therefore, time is required for the stresses to redistribute to the steady-state creep stress distribution controlled by C^*. In addition, a period of time is needed for creep damage to develop around the crack tip [9]. During this period, transient conditions exist which are not uniquely defined by C^*. Furthermore due to the practical limitations of crack detection equipment, the initiation of crack growth is difficult to determine precisely. Typically, this ranges between an extension Δa of between about 0.1 and 0.5 mm depending on component and crack dimensions. ASTM E1457-01 [i] identifies an extension of 0.2 mm for tests on C(T) specimens to cover the entire transition time to steady state conditions. This distance also takes into account the resolution of crack monitoring equipment. In this procedure, it has been determined that time to Δa=0.5 mm is a suitable value to adopt as an 'engineering' limit for CCI in fracture mechanics geometries. From Equation (1) it may be expected that the time, t_i, to initiate a crack extension of Δa can be expressed as giving:

$$t_i = D_i \cdot C^{*\phi_i} \qquad (14)$$

where D_i and ϕ_i are material constants. For steady-state cracking D_i is expected to be given approximately by $\Delta a / D$ with $\phi_i = -\phi$ and hence Equation (14) can be re-written as follows:

$$t_i = \frac{\Delta a}{D} \cdot C^{*-\phi_i} \qquad (15)$$

These equations assume that the entire initiation period is governed by steady state C^*. This cannot be expected to be true during at least part of the initiation period t_i. For the CCI correlation, the time to 0.5 mm crack growth versus C^* or K should be plotted and for CCG correlation a plot of crack growth rate, da/dt, as a function of C^* or K should be presented after Section 9 has be used to validate the results.

11.3 FCG rate Analysis

For fatigue crack growth it is assumed that the mechanism is time and temperature independent. At room temperature under cyclic loading conditions, crack propagation usually occurs by a fatigue mechanism where the Paris Law can describe crack growth/cycle $(da/dN)_f$ in terms of stress intensity factor range ΔK by

$$(da/dN)_f = C' \Delta K^{m'} \qquad (16)$$

Where *da/dN* is fatigue crack growth rate per cycle, *C'* and *m'* are material dependent parameters, which may be sensitive to the minimum to maximum load ratio *R* of the cycle. At elevated temperatures combined creep and fatigue crack growth may take place.

11.4 Creep/fatigue crack growth rate analysis

In most cases the crack growth rate at elevated temperature is described in terms of Equation (13). The cracking per cycle due to fatigue is calculated from the Equation (16). The predictions made using these equations may be over conservative where the stresses at one end of the cycle are compressive. If the margins against failure are insufficient, the fatigue crack growth calculations can be refined using the method given in the British Energy's R5 Procedure. Total crack growth per cycle, (*da/dN*), is given by

$$(da/dN) = (da/dN)_C + (da/dN)_f \qquad (17)$$

Where this linear summation combines creep and creep/fatigue components. Previous studies [20] have shown that a simple cumulative damage law can be applied to describe creep/fatigue interactions.

12 Methods for Calculating the *C** Parameter

The *C** parameter may be estimated in different ways. These include analytical, numerical, experimental or a combination of these. With laboratory testspieces where the load-defection can be measured it has been found that an experimental measure for the parameter conveniently and accurately estimates *C**. Whereas for feature components the reference stress method (see Section 12.2) has been adopted as the method of choice. Ideally if the right input values for uniaxial material properties are used the two methods should give the same *C** values. In practice this is not usually the case. The 'Benchmark' material properties data is taken as the *C** which has been derived from the experimental methods as described also in ASTM E1457 [i]. As the measured displacement rate is an instantaneous measure of the material/geometry response at the crack tip it is assumed that the derived *C** using Equation (18) gives an accurate reflection of the crack-tip stresses. Any deviation from these properties with respect to *C** experimental, therefore, must be explained in terms of differences in material uniaxial properties used, and effects of constraint due to size and geometry. A short description for the C* derivations follow in Sections 12.1and 12.2.

Note 11: It should be noted that for the geometries shown in APPENDIX I the values derived by the two methods were found to be at worst within a factor of 2.

12.1 Experimental Estimates of *C**

Directly, C* may be determined from the creep load-line displacement rate. Estimates of *C** can be obtained by experimental, numerical and limit analysis methods. Following ASTM E1457-01 *C** is given by the following equation:

$$C^* = \frac{P\dot{\Delta}}{B_n(W-a)}F' \qquad (18)$$

where *P* is the applied load, *W-a* is the remaining ligament ahead of the crack and B_n is the net thickness (= *B* for a specimen without side grooves) and F' is a function of the materials creep properties and a geometric factor. The details of estimating F' for different geometries are given in

Section 13. In APPENDIX I all the relevant information is given to calculate the parameters described in this Section. In Equation (18) $\dot{\Delta}$ is the measure load-line displacement rate and is ideally used as $\dot{\Delta}^c \cong \dot{\Delta}$ where $\dot{\Delta}^c$ (the creep displacement rate). This assumes small amounts of elastic and plastic components giving the corresponding rates as approximately:

$$\dot{\Delta}^c = \dot{\Delta}^t - \dot{\Delta}^e - \dot{\Delta}^p \approx \dot{\Delta}^t - \frac{aB_n}{P}\left[\frac{2K^e}{E'}\right] \qquad (19)$$

where $\dot{\Delta}^t$, $\dot{\Delta}^e$ and $\dot{\Delta}^p$ are the total, the elastic and the plastic displacement rates respectively. Creep crack growth testing is normally carried out at loads where plastic deformation is insignificant and in any event the presence of plasticity assists the redistribution of crack tip stresses in the same manner as C^*. Also for lengths of crack extensions (usually1-10 mm) that have been observed in the geomteries listed in Section 13 it is found that the range of the elastic portion of displacement $\Delta^e << \Delta^c$ in creep ductile conditions. It is therefore appropriate that for most practical test conditions in extensive creep conditions [24,54] it can be assumed that $\dot{\Delta}^e >> \dot{\Delta}^p$ and $\dot{\Delta}^c >> \dot{\Delta}^e$. Hence the creep strain rate where creep is dominant is calculated as $\dot{\Delta}^t$ making

$$\dot{\Delta}^c \cong \dot{\Delta}^t \qquad (20)$$

The errors involved in this assumption are at most a factor of 2 for creep which falls well within the experimental scatter inherent in CCG data which have been found to be as much as a factor of 5 in any given one batch [64-69]. This simplification therefore is not expected to affect the overall results and comparisons in the CCI and CCG or CFFG rate analyses using C^*.

12.2 Reference Stress Method of Estimating C^*

Where load-line deformation rates are not available the proposed method, which has been widely adopted in life assessment codes [30-35], is one based on the reference stress concepts (see Section 12.2). Reference stress procedures are employed to evaluate C^* for feature and actual component tests where the load-line deformation rate is not a measurable quantitatively) by determining;

$$C^* = \sigma_{ref} . \dot{\varepsilon}_{ref} \left(\frac{K}{\sigma_{ref}}\right)^2 \qquad (21)$$

Where $\dot{\varepsilon}_{ref}$ is the creep strain rate at the reference stress, σ_{ref} and K is the stress intensity factor. Usually it is most convenient to employ limit analysis to obtain $\sigma_{ref} = \sigma_y(P/P_{lc})$, where P_{lc} is the collapse load of a cracked body and σ_y is the yield stress. The value of P_{lc} will depend on the collapse mechanism assumed and whether plane stress or plane strain conditions apply. σ_{ref} can be derived from either limit load solutions [71-73] or directly from numerical calculations using elastic/plastic finite element analysis. When the creep strain rate $\dot{\varepsilon}$ at an applied stress σ can be described in terms of the Norton's creep law:

$$\dot{\varepsilon} = A \cdot \sigma^n \qquad (22)$$

where A and n are material constants at constant temperature. Thus, Equation (21) can be rewritten as

$$C^*_{ref} = A \cdot \sigma^{n-1}_{ref} \cdot K^2 \tag{23}$$

The typical value for n is between 5 and 12 for most metals. In addition, the concept of the average creep rate, $\dot{\varepsilon}_{Ave}$, obtained directly from rupture data, has been proposed [9] to account for all three stages of creep as an approximate method for estimating the average creep rate $\dot{\varepsilon}_{Ave}$. Hence the average creep rate, $\dot{\varepsilon}_A$, is described schematically and is defined by

$$\dot{\varepsilon}_A = \frac{\varepsilon_f}{t_r} = \dot{\varepsilon}_o \left(\frac{\sigma}{\sigma_0} \right)^{n_A} = A_A \sigma^{n_A} \tag{24}$$

where ε_f is the uniaxial failure strain, t_r is the time to rupture and σ is the applied stress. The variables $\dot{\varepsilon}_o$, σ_o, A_A and n_A may be taken as material constants. When Equation (24) is used in the analysis to estimate C^* it is found that the value of C^* could increase by as much as a factor of 2-3. Therefore depending on the level of conservatism that the user is seeking in remaining life assessment the use of Equation (24) is likely to predict the shorter lives compare to the minimum strain rates.

13 APPENDIX I

13.1 Test Specimen Geometries

In this Section the geometry definitions for standard laboratory specimens and feature component tests are presented. The fracture mechanics functions used in the analysis Section are also provided for each specimen.

13.2 Geometry Definitions for Laboratory Specimens

This CoP identifies seven specimen geometries that have been verified for the purpose of CCI, CCG and CFCG testing. This does not mean that different variations of geometries are invalid but that they may need further verification. This annex presents the geometries, dimensions and machining instructions for the geometries listed below. Figure A.I.2 show the schematic figures, engineering drawings and suggested displacement measuring positions respectively. The dimension suggested in Table A.I.1 for specimen sizes would give applied loads between 10-50 kN depending on crack lengths, sidegrooving B_n (between 10-20% (each side), see Section 8.3.5) and thickness and have been found to be a practical size for testing.

The abbreviations which are to be used to denote the specimen geometries examined are given in Table A.I.1.

Table A.I.1: Specimen abbreviations and allowed relative sizes

		W mm	*B mm*	*H. L, R_0 (mm)*
C(T)	Compact Tension	50	*W/2→W/4*	*H=1.2W*
CS(T)	C-Shaped Tension	25	*W/2→W/4*	*R=2W*
SEN(T)	Single Edge Notched Tension	25	*W/2→W/4*	*L=2W*
SEN(B)	Single Edged Notched Bending	25	*W/2→W/4*	*L=2W*
DEN(T)	Double Edge Notched Tension	25	*W/2→W/4*	*L=2W*
M(T)	Middle Tension	25	*W/2→W/4*	*L=2W*

Where H is half height of C(T), R_0 is the outer radius of CS(T) and L is the half length of SEN (T).SEN (B), DEN(T) and M(T) specimens. Allowable sidegrooving B_n (between 10-20% on eaqch side) to produce a straight-fronted crack. An illustration of each specimen geometry is shown in Figure A.I.2. In this figure the specimen dimensions are defined together with the loading configuration. The load line displacement, Δ^{LLD}, and crack mouth opening displacement, Δ^{CMOD}, of an arbitrary pin loaded geometry are defined in Figure A.I.2 shows a schematic of a SEN(T) specimen (a) pin-loaded and (b) loaded under uniform displacement.

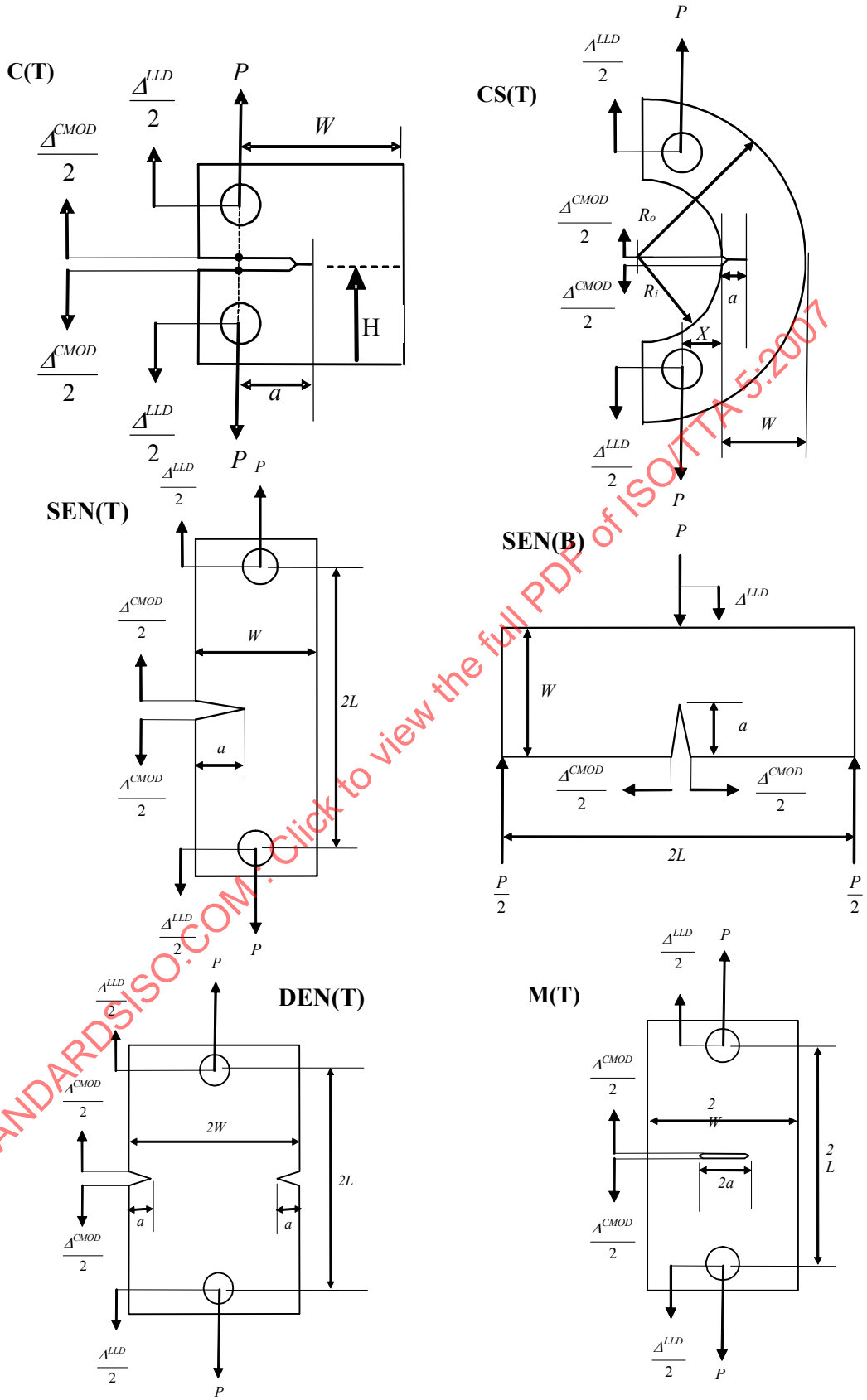

Figure A.I.2: Schematic drawings for the fracture mechanics geometries showing the loading directions, and the load-line (LLD) and crack Mouth opening (CMOD) measuring positions

14 SPECIMEN FRACTURE MECHANICS PARAMETER SOLUTIONS

In this Section a detailed list of fracture mechanics parameters *(K, C*, η, σ_{ref})* used in the analysis of the data are presented for the specific geometries quoted in Section 13. These are verified solutions which can be used in the analysis of creep and creep/fatigue crack growth data.

14.1 Stress Intensity Factor *K*

The linear elastic K is appropriate for creep brittle analysis (see Section 9.3.4), cycle dependent fatigue (see Section 7.5.1) as well as for estimating C^* for components (see Section 14.9) and also K^c_{mat} (see Section 15) and Q^* (see Section 16). Therefore it is important to have an accurate measure of K. Fortunately there are numerous references which tabulate or quote K values for different components [55-58].

The general equation for stress intensity factor is given by

$$K = Y\left(a/W\right)\sigma\sqrt{a} \qquad \text{(A.I.25)}$$

where σ the applied nominal stress and $Y(a/W)$ is a function of geometry and a, crack length and W, geometry width, as defined in Figure A.I.2. When a specimen is side-grooved, the applied load will be acting over a shorter crack front and the stress intensity factor of a side-grooved specimen K_n, is given by

$$K_n = K\sqrt{\frac{B}{B_n}} \qquad \text{(A.I.26)}$$

where B_n is the net specimen thickness.
Equations (A.I.29) to (A.I.43) also include equations the membrane bending moments for specimens loaded under a tensile load P and for specimens subjected to a constant bending moment M the nominal bending stress at the surface.

Where analytical expressions do not exist or where an alternative solution is sought K can be calculated from the associated EPRI J [59] integral:

$$K = \sqrt{EJ_{el}} \qquad \text{(A.I.27)}$$

where $J_{el} = J_{N=1}$ given by the following formula:

$$J = \sigma_o \varepsilon_o (W-a) h_1 \left(\frac{P}{P_o}\right)^{N+1} \qquad \text{(A.I.28)}$$

where P_o is the limit load and the h_1 functions are tabulated in the literature [59].

14.2 Solutions for the *Y* function

Solutions for the function Y and σ for the geometries listed in APPENDIX I Section 13 are given below.

14.2.1 *Y factor for C(T)*

$$Y = \sqrt{\frac{W}{a}}\left[\frac{2 + a/W}{(1-a/W)^{3/2}}\right] f(a/W) \tag{A.I.29}$$

$$f(a/W) = 0.886 + 4.64(a/W) - 13.32(a/W)^2 + 14.72(a/W)^3 - 5.6(a/W)^4 \tag{A.I.30}$$

$$\sigma = \frac{P}{BW} \tag{A.I.31}$$

14.2.2 *Y factor for CS(T)*

$$Y = \sqrt{\frac{W}{a}}\left[\frac{3X}{W} + 1.9 + 1.1\left(\frac{a}{W}\right)\right]\left[1 + 0.25\left(1-\frac{a}{W}\right)^2\left(1-\frac{R_i}{R_o}\right)\right] f(a/W) \tag{A.I.32}$$

$$f(a/W) = \frac{\sqrt{a/W}}{(1-a/W)^{3/2}}\left(3.74 - 6.3(a/W) + 6.32(a/W)^2 - 2.43(a/W)^3\right) \tag{A.I.33}$$

$$\sigma = \frac{P}{BW} \tag{A.I.34}$$

where R_i and R_o are the inner and outer radii, respectively, and X is the loading hole offset, as defined in Figure A.1.2.

14.2.3 *Y factor for for SEN(T)*

$$Y = \sqrt{\frac{2W}{a}\tan\left(\frac{\pi a}{2W}\right)}\left[0.752 + 2.02\left(\frac{a}{W}\right) + 0.37\left(1 - \sin\left(\frac{\pi a}{2W}\right)^3\right)\right] \Big/ \cos\left(\frac{\pi a}{2W}\right) \tag{A.I.35}$$

$$\sigma = \frac{P}{BW} \tag{A.I.36}$$

14.2.4 *Y factor for SEN(B) (3 Point Bend Specimen)*

For Span = $4W$ *i.e.* $L/W = 2$

$$Y = \frac{1}{(1+2a/W)(1-a/W)^{3/2}}\left[1.99 - \frac{a}{W}\left(1-\frac{a}{W}\right)\left(2.15 - 3.93\frac{a}{W} + 2.7\left(\frac{a}{W}\right)^2\right)\right] \tag{A.I.37}$$

$$\sigma = \frac{3PL}{BW^2} \tag{A.I.38}$$

14.2.5 *Y factor for DEN(T)*

$$Y = \sqrt{\frac{2W}{a}\tan\left(\frac{\pi a}{2W}\right)}\left[1+0.122\cos^4\left(\frac{\pi a}{2W}\right)\right] \quad \text{(A.I.39)}$$

$$\sigma = \frac{P}{2BW} \quad \text{(A.I.40)}$$

For DEN(T) specimen the width W is replaced by $2W$.

14.2.6 *Y factor for M(T)*

$$Y = \sqrt{\pi\sec\left(\frac{\pi a}{2W}\right)}\left[1-0.25\left(\frac{a}{W}\right)^2+0.06\left(\frac{a}{W}\right)^4\right] \quad \text{(A.I.41)}$$

$$\sigma = \frac{P}{2BW} \quad \text{(A.I.42)}$$

14.3 *C** Solutions

Estimates of C^* can be obtained by experimental analysis methods as outlined in Section 12.1. The experimental procedure is applicable to laboratory specimens as specified in this document as shown in Section 13. Experimentally C^* is calculated from the general relationship,

$$C^* = (P\dot{\Delta}\ /(W-a)B_n)F' \quad \text{(A.I.43)}$$

where $\dot{\Delta}$ is the load-line displacement rate (see Section 12.1), F is a non-dimensional factor which is a function the uniaxial creep properties n and a geometry dependant factor (which can be obtained from limit analysis techniques), B_n is the net thickness of the specimen with side-grooves and W is the width. In general, Equation (A.I.43) is used to estimate the values of C^* using $\dot{\Delta} = \dot{\Delta}^t$ (see Section 12.1) for tests in the laboratory.

The factor F' can be given by,

$$F' = -\frac{n}{n+1}\frac{W}{P_L}\frac{dP_L}{da} = -\frac{n}{n+1}\frac{1}{m}\frac{dm}{d(a/W)} \quad \text{(A.I.44)}$$

Where m is the yield load ratio and P_L is the limit load. Hence, C^* can be re-expressed as

$$C^* = \frac{P\dot{\Delta}}{B_n(W-a)}\frac{n}{n+1}\eta \quad \text{(A.I.45)}$$

where

$$\eta = -\frac{1}{m}\frac{dm}{d(a/W)} \quad \text{(A.I.46)}$$

The η functions from Equation (A.I.46) for each geometry can be derived analytically which has been found to be unsatisfactory [77]. Using the Finite Element method to derive η [63] for the geometries shown in Figure A.1.2 a more accurate representation of η is derived. The results of these calculations are given in Equations (A.I.65) to (A.I.92). This allow solutions for C^* to be derived from η calculated from elastic-plastic FE analysis (see Section 14.6), and the experimental load-line displacement rate. For this reason the expression for C^* given in Equation (A.I.43) is referred to as experimental C^*.

14.4 Reference Stress (σ_{ref}) Solutions

A general expression for the reference stress, σ_{ref}, of a structure subjected to a tensile load may be written as

$$\sigma_{ref} = \frac{P}{P_{LC}}\sigma_0 \qquad \text{(A.I.47)}$$

where P is the applied load, P_{LC} is the limit load value of a cracked body of yield stress σ_0.

Limit load solutions are given below based on the von Mises yield criterion for both plane stress and plane strain conditions, enabling the reference stress, σ_{ref}, to be obtained from Equation (A.I.47). Where necessary, the limit load solution is validity range in terms of crack length to specimen width ratio, a/W, is specified. Solutions are given for plain sided specimens of thickness, B. For side-grooved specimens B should be replaced by the net-section thickness, B_n, or by the effective thickness B_{eff} given by

$$B_{eff} = B_n\left(2 - \frac{B_n}{B}\right). \qquad \text{(A.I.48)}$$

The following common notation is used

$$x = \frac{a}{W},\ y = 1 - \frac{a}{W};\ \gamma = \frac{2}{\sqrt{3}}. \qquad \text{(A.I.49)}$$

14.4.1 σ_{ref} for C(T)

$$\frac{P_{LC}}{BW\sigma_0} = \begin{cases} -(1+\gamma x) + \sqrt{(1+\gamma)(1+\gamma x^2)} & \text{Plane Stress} \quad \text{(A.I.50)} \\ \gamma\left[-(1+1.702x) + \sqrt{2.702(1+1.702x^2)}\right] & \text{Plane Strain} \quad \text{(A.I.51)} \end{cases}$$

14.4.2 σ_{ref} for CS(T)

$$\frac{P_{LC}}{BW\sigma_0} = \begin{cases} -\gamma\left(\frac{1}{2}+x\right)-\frac{3}{2}+\sqrt{\frac{1}{4}\left[\gamma(1+2x)+3\right]^2+(1-x)^2} & \text{Plane Stress} \quad \text{(A.I.52)} \\ 1.26\gamma\left(-\gamma\left(\frac{1}{2}+x\right)-\frac{3}{2}+\sqrt{\frac{1}{4}\left[\gamma(1+2x)+3\right]^2+(1-x)^2}\right) & \text{Plane Strain} \quad \text{(A.I.53)} \end{cases}$$

14.4.3 σ_{ref} for SEN(T)

$$\frac{P_{LC}}{BW\sigma_0} = \begin{cases} 1-x-x^2 & x<0.146 \\ \sqrt{\left(\frac{\gamma+1}{2}\right)^2-\gamma(1+\gamma)xy}-\gamma x+\frac{\gamma-1}{2} & x>0.146 \quad \text{Plane Stress} \quad \text{(A.I.54)} \\ \gamma\left(1-x-1.232x^2+x^3\right) & x\le 0.545 \\ 1.702\gamma\left[\begin{matrix}-0.794+y \\ +\sqrt{0.794-y^2+0.5876y^2}\end{matrix}\right] & x>0.545 \quad \text{Plane Strain} \quad \text{(A.I.55)} \end{cases}$$

14.4.4 σ_{ref} for SEN(B) (3 Point Bend Specimen)

$$\frac{2P_{LC}}{BW^2\sigma_0} = \begin{cases} 1.072y^2 & x>0.154 \quad \text{Plane Stress} \quad \text{(A.I.56)} \\ 1.218\gamma y^2 & x>0.177 \quad \text{Plane Strain} \quad \text{(A.I.57)} \end{cases}$$

14.4.5 σ_{ref} for DEN(T)

$$\frac{P_{LC}}{2BW\sigma_0} = \begin{cases} (1+0.54x)\,y & x\le 0.286 \quad \text{Plane Stress} \quad \text{(A.I.58)} \\ \gamma y & x>0.286 \\ \gamma y\left[1+\ln\left(\frac{1-x/2}{y}\right)\right] & x<0.884 \quad \text{Plane Strain} \quad \text{(A.I.59)} \end{cases}$$

14.4.6 σ_{ref} *for M(T)*

$$\frac{P_{LC}}{2BW\sigma_0} = \begin{cases} y & \text{Plane Stress} \quad \text{(A.I.60)} \\ \gamma y & \text{Plane Strain} \quad \text{(A.I.61)} \end{cases}$$

14.5 η Functions for cracked geometries

The η functions, used to evaluate C^* (see Section 14.3), have been derived and validated [73-74] for the fracture mechanics specimens shown in Figure A.I.2. The results have been derived from numerous finite element studies which have calculated η for a range of conditions such as different mesh sizes, specimen dimensions and loading boundary conditions, plane stress/strain conditions, materials with a range uniaxial creep properties with creep indices n between 3-20. As it was found that no single trend existed between these variable the best linear values of η for appropriate range of crack lengths were chosen. The deviations from the mean were found to be about ±50% for $a/W <$ 0.3 and ±25% for $a/W >$ 0.3. This suggests that testing short crack length is likely to give a wider scatter compared to long crack lengths. DEN(T) is the exception where there is a wider divergence at long crack lengths compared to short crack length. The mean values for η are given as Equations (A.I.65)-(A.I.92) and are also in a tabulated with respect to C^* as η^{LLD} (**Table A.I. 2**) and η^{CMOD} (**Table A.I.3**) with respect to crack length.

14.5.1 *Nomenclature (see Figure A.I.3)*

a	Crack length
$\dot{a}$	Crack growth rate
B	Specimen thickness
B_n	Specimen thickness between side-grooves
C^*	Experimentally determined value of C^* parameter
E	Elastic modulus
E'	Effective elastic modulus, $E/(1-\nu^2)$ for plane strain and E for plane stress
F	Geometric function
F^{LLD}, F^{CMOD}	Geometric function derived from LLD or CMOD displacements
L	Specimen half length
n	Power-law creep stress exponent ($\dot{\varepsilon} \propto \sigma^n$)
P	Applied load
R_o	Outer radius of CS(T) specimen
R_i	Inner radius of CS(T) specimen
W	Specimen width or half width
Δ^{LLD}, $\dot{\Delta}^{LLD}$	Load line displacement, load line displacement rate
$\dot{\Delta}_c^{LLD}$	Component of the load line displacement rate directly associated with the accumulation of creep strains
$\dot{\Delta}_i^{LLD}$	Component the load line displacement rate directly associated with instantaneous strains
Δ^{CMOD}, $\dot{\Delta}^{CMOD}$	Crack mouth opening displacement, crack mouth opening displacement rate
η^{LLD}	Geometric factor to calculate C^* from load line displacement rate

η^{CMOD} Geometric factor to calculate C^* from CMOD rate
v Poisson's ratio

14.5.2 *Solutions for creep crack growth parameter, C**

C^* can be calculated, as previously stated in Section 12, from the load-line displacement rate or crack mouth opening displacement rate using the following equations

$$C^* = \frac{P\dot{\Delta}^{LLD}}{B(W-a)} F^{LLD}\eta^{LLD} \qquad \text{(A.I.62)}$$

or

$$C^* = \frac{P\dot{\Delta}^{CMOD}}{B(W-a)} F^{CMOD}\eta^{CMOD} \qquad \text{(A.I.63)}$$

Solutions for the functions F^{LLD}, F^{CMOD}, Δ^{LLD} and Δ^{CMOD} for test specimens are given in Equations (A.I.65) to (A.I.92).

Solutions are given for plain sided specimens of thickness, B. For side-grooved specimens B in Equations (A.I.62) and (A.I.63) should be replaced by B_n (as shown in Figure A.I.3 and Figure A.I.4).

The Δ^{LLD} and Δ^{CMOD} are provided as a function of relative crack depth, a/W. For some crack geometries, the value of Δ^{LLD} and Δ^{CMOD} is sensitive to the creep exponent, n, and relative specimen height, L/W. This variability has been taken into account here through the use of a mean value for a range of n and L/W values and an uncertainty which quantifies the potential variability in Δ^{LLD} and Δ^{CMOD} as a function of geometry and material. Calculated values of η^{LLD} and η^{CMOD} for specific values of a/W are given in Tables respectively.

The load line displacement rate, $\dot{\Delta}^{LLD}$, can be partitioned into an instantaneous (elastic) part, $\dot{\Delta}_i^{LLD}$, and a time-dependent part that is directly associated with the accumulation of creep strains, $\dot{\Delta}_c^{LLD}$. The instantaneous load line displacement rate is calculated as

$$\dot{\Delta}_i^{LLD} = \frac{\dot{a}B}{P}\left[\frac{2K^2}{E'}\right] \qquad \text{(A.I.64)}$$

where $\dot{a}$ is the crack growth rate, P is the applied load, B is the specimen thickness, K is the stress intensity factor, and E' is the effective elastic modulus ($E/(1\text{-}v^2)$ for plane strain and E for plane stress). For side-grooved specimens B in Eq. (A.I.64) should be replaced by B_n.

In Equation (A.I.62) $\dot{\Delta}^{LLD}$ and $\dot{\Delta}^{CMOD}$ are the total load line and crack mouth opening displacement rates, respectively. Thus it is assumed that steady state, extensive creep conditions prevail, and that the data can be classified as being creep-ductile (i.e. $\dot{\Delta}_c^{LLD} / \dot{\Delta}^{LLD} \geq 0.5$).

14.5.3 *Best fit solutions of η from finite element calculations*

The numerically driven solutions of η-factors for a range of fracture mechanics geometries (shown in Figure A.I.2) are presented in this document. The load-line displacement η^{LLD} and the crack mouth opening displacement η^{CMOD} are presented with respect to normalised crack length a/W. The results are derived from numerous analyses and cover a range of creep properties and stress states [73,76]. The values of η^{LLD} (**Table A.I. 2**) and η^{CMOD} (**Table A.I.3**) or Equations (A.I.65) to (A.I.92) are the mean values and advice is given in Sections 14.5.4 and 14.5.5 on the appropriate use of the factors.

Note 12: It should also be possible also to derive C^* for 'feature' components (examples of which are shown in Figure A.I.4) once the η functions for the CMOD have been calculated and verified.

14.5.4 *Choice of η for evaluating C* for material CCI and CCG properties*

For material CCI, CCG and CFCG properties with respect to C^* the mean values of η^{LLD} (**Table A.I. 2**) and η^{CMOD} (**Table A.I.3**) or Equations (A.I.65) to (A.I.92) should be used. These are recommended values that can be used to calculate both J and C^* solutions for the range of crack lengths shown.

14.5.5 *Choice of η for evaluating C* in life assessment*

For increased conservatism in C^* calculations when performing remaining life assessment using Equation (A.I.62) the values of η may be multiplied by 25% for crack lengths of $a/W > 0.3$ and by 50% for crack lengths of $a/W < 0.3$, to take into consideration unknowns such as material creep properties, plane stress/strain conditions at the crack tip and variation the dimensions from the norm. There is a direct proportionality between η and C^* (see Section 12) and therefore the effect due to the unknowns in η is well below the ranger of experimental scatter observed in the data.

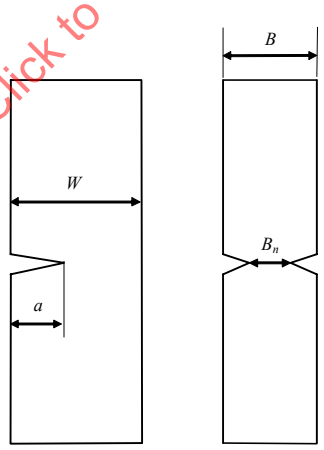

Figure A.I.3: Generic edge cracked specimen defining B and B_n.

14.6 η Function Equations

14.6.1 η *functions for C(T)*

$$F^{LLD} = \frac{n}{n+1} \qquad \text{(A.I.65)}$$

$$\eta^{LLD} = 2.2 \qquad 0.4 \le x \le 0.7 \qquad \text{(A.I.66)}$$

$$\eta^{CMOD} = 2.2 \qquad 0.4 \le x \le 0.7 \qquad \text{(A.I.67)}$$

14.6.2 η *functions for CS(T)*

$$F^{LLD} = \frac{n}{n+1} \qquad \text{(A.I.68)}$$

$$\eta^{LLD} = 7a/W - 0.64 \qquad 0.2 \le x < 0.4 \qquad R_i/R_o = 0.5 \qquad \text{(A.I.69)}$$

$$\eta^{LLD} = 0.4a/W + 2 \qquad 0.4 \le x \le 0.55 \qquad X/W = 0.5 \qquad \text{(A.I.70)}$$

$$\eta^{LLD} = 4.6 - 1.6a/W \qquad 0.2 \le x \le 0.55 \qquad R_i/R_o = 0.5 \quad X/W = 0.5 \qquad \text{(A.I.71)}$$

14.6.3 η *functions for SEN(T)*

$$F^{LLD} = \frac{n}{n+1} \qquad \text{(A.I.72)}$$

$$\eta^{LLD} = 5.0x - 0.06 \qquad 0.1 \le x \le 0.5 \quad 1 \le L/W \le 3 \qquad \text{(A.I.73)}$$

$$\eta^{LLD} = 2.44 \qquad 0.5 < x \le 0.7 \quad 1 \le L/W \le 3 \qquad \text{(A.I.74)}$$

$$F^{CMOD} = \frac{n}{n+1} \qquad \text{(A.I.75)}$$

$$\eta^{CMOD} = 1.0 \qquad 0.1 \le x \le 0.7 \quad 1 \le L/W \le 4 \qquad \text{(A.I.76)}$$

14.6.4 *η functions for SEN(B) — 3PB*

$$F^{LLD} = \frac{n}{n+1} \qquad \text{(A.I.77)}$$

$$\eta^{LLD} = 4.06x + 0.60 \qquad 0.1 \le x \le 0.3 \qquad \text{(A.I.78)}$$

$$\eta^{LLD} = 0.56x + 1.65 \qquad 0.3 < x \le 0.7 \qquad \text{(A.I.79)}$$

$$F^{CMOD} = \frac{2L}{W}\frac{n}{n+1} \qquad \text{(A.I.80)}$$

$$\eta^{CMOD} = 0.92 - 0.46x \qquad 0.1 \le x \le 0.7 \qquad \text{(A.I.81)}$$

14.6.5 *η functions for DEN(T)*

$$F^{LLD} = \frac{n-1}{2(n+1)} \qquad \text{(A.I.82)}$$

$$\eta^{LLD} = 1.43x + 0.15 \qquad 0.1 \le x \le 0.3 \quad 2 \le L/W \le 4 \qquad \text{(A.I.83)}$$

$$\eta^{LLD} = 0.53x + 0.42 \qquad 0.3 < x \le 0.7 \quad 2 \le L/W \le 4 \qquad \text{(A.I.84)}$$

$$F^{CMOD} = \frac{n-1}{2(n+1)} \qquad \text{(A.I.85)}$$

$$\eta^{CMOD} = 1.26 - 0.80x \qquad 0.1 \le x < 0.5 \quad 2 \le L/W \le 6 \qquad \text{(A.I.86)}$$

$$\eta^{CMOD} = 0.86 \qquad 0.5 \le x \le 0.7 \quad 2 \le L/W \le 6 \qquad \text{(A.I.87)}$$

14.6.6 *η functions for M(T)*

$$F^{LLD} = \frac{n-1}{2(n+1)} \qquad \text{(A.I.88)}$$

$$\eta^{LLD} = 2.32x + 0.18 \qquad 0.1 \le x \le 0.35 \qquad \text{(A.I.89)}$$

$$2 \le L/W \le 4$$

$$\eta^{LLD} = 0.99 \qquad 0.35 < x \le 0.7 \qquad \text{(A.I.90)}$$

$$2 \le L/W \le 4$$

$$F^{CMOD} = \frac{n-1}{2(n+1)} \qquad \text{(A.I.91)}$$

$$\eta^{CMOD} = 1.26x - 0.36 \qquad 0.1 \le x \le 0.7 \qquad \text{(A.I.92)}$$

$$2 \le L/W \le 6$$

14.7 Table for η^{LLD}

Table A.I. 2: Calculated values of η^{LLD} for specific values of a/W

	η^{LLD}					
a/W	SEN(T)	M(T)	DEN(T)	SEN(B)	C(T)	CS(T)
0.10	0.44	0.41	0.29	1.01	—	—
0.12	0.54	0.46	0.32	1.09	—	—
0.14	0.64	0.50	0.35	1.17	—	—
0.16	0.74	0.55	0.38	1.25	—	—
0.18	0.84	0.60	0.41	1.33	—	—
0.20	0.94	0.64	0.44	1.41	—	0.76
0.22	1.04	0.69	0.46	1.49	—	0.90
0.24	1.14	0.74	0.49	1.57	—	1.04
0.26	1.24	0.78	0.52	1.66	—	1.18
0.28	1.34	0.83	0.55	1.74	—	1.32
0.30	1.44	0.88	0.58	1.82	—	1.46
0.32	1.54	0.92	0.59	1.83	—	1.60
0.34	1.64	0.97	0.60	1.84	—	1.74
0.36	1.74	0.99	0.61	1.85	—	1.88
0.38	1.84	0.99	0.62	1.86	—	2.02
0.40	1.94	0.99	0.63	1.87	2.20	2.16
0.42	2.04	0.99	0.64	1.89	2.20	2.17
0.44	2.14	0.99	0.65	1.90	2.20	2.18
0.46	2.24	0.99	0.66	1.91	2.20	2.18
0.48	2.34	0.99	0.67	1.92	2.20	2.19
0.50	2.44	0.99	0.69	1.93	2.20	2.20
0.52	2.44	0.99	0.70	1.94	2.20	2.21
0.54	2.44	0.99	0.71	1.95	2.20	2.22
0.56	2.44	0.99	0.72	1.96	2.20	—
0.58	2.44	0.99	0.73	1.97	2.20	—
0.60	2.44	0.99	0.74	1.99	2.20	—
0.62	2.44	0.99	0.75	2.00	2.20	—
0.64	2.44	0.99	0.76	2.01	2.20	—
0.66	2.44	0.99	0.77	2.02	2.20	—
0.68	2.44	0.99	0.78	2.03	2.20	—
0.70	2.44	0.99	0.79	2.04	2.20	—

14.8 Table for η^{CMOD}

Table A.I.3: Calculated values of η^{CMOD} for specific values of a/W

	η^{CMOD}					
a/W	SEN(T)	M(T)	DEN(T)	SEN(B)	C(T)	CS(T)
0.10	1.00	1.22	1.18	0.87	—	—
0.12	1.00	1.22	1.16	0.86	—	—
0.14	1.00	1.21	1.15	0.86	—	—
0.16	1.00	1.20	1.13	0.85	—	—
0.18	1.00	1.20	1.12	0.84	—	—
0.20	1.00	1.19	1.10	0.83	—	4.28
0.22	1.00	1.18	1.08	0.82	—	4.25
0.24	1.00	1.17	1.07	0.81	—	4.22
0.26	1.00	1.17	1.05	0.80	—	4.18
0.28	1.00	1.16	1.04	0.79	—	4.15
0.30	1.00	1.15	1.02	0.78	—	4.12
0.32	1.00	1.14	1.00	0.77	—	4.09
0.34	1.00	1.14	0.99	0.76	—	4.06
0.36	1.00	1.13	0.97	0.75	—	4.02
0.38	1.00	1.12	0.96	0.75	—	3.99
0.40	1.00	1.12	0.94	0.74	2.20	3.96
0.42	1.00	1.11	0.92	0.73	2.20	3.93
0.44	1.00	1.10	0.91	0.72	2.20	3.90
0.46	1.00	1.09	0.89	0.71	2.20	3.86
0.48	1.00	1.09	0.88	0.70	2.20	3.83
0.50	1.00	1.08	0.86	0.69	2.20	3.80
0.52	1.00	1.07	0.86	0.68	2.20	3.77
0.54	1.00	1.07	0.86	0.67	2.20	3.74
0.56	1.00	1.06	0.86	0.66	2.20	—
0.58	1.00	1.05	0.86	0.65	2.20	—
0.60	1.00	1.04	0.86	0.64	2.20	—
0.62	1.00	1.04	0.86	0.63	2.20	—
0.64	1.00	1.03	0.86	0.63	2.20	—
0.66	1.00	1.02	0.86	0.62	2.20	—
0.68	1.00	1.02	0.86	0.61	2.20	—
0.70	1.00	1.01	0.86	0.60	2.20	—

14.9 Geometry Definitions for 'Feature' Type Specimens

This Section only gives details and information on geometries that have been tested and analysed [21,29,38-41,50,52] and will therefore not list the wider range of 'feature geometries' that may be possible. However the user is not restricted in testing and analyse new geometries providing appropriate stress intensity factors, reference stress solutions and material properties are available or can be accessed in the literature from sources such as in R5 [31] or API 579 [35].

14.9.1 *Details form Pipe, Plate and Notched bar 'feature specimens'*

In this Section the geometry definitions for 'feature' specimens are presented as shown in Figure A.I.4. It is usual that for most cases only a few test of this kind would be attempted and therefore they normally serve the purpose of bridging the information gap between standard laboratory testpieces and the real component.

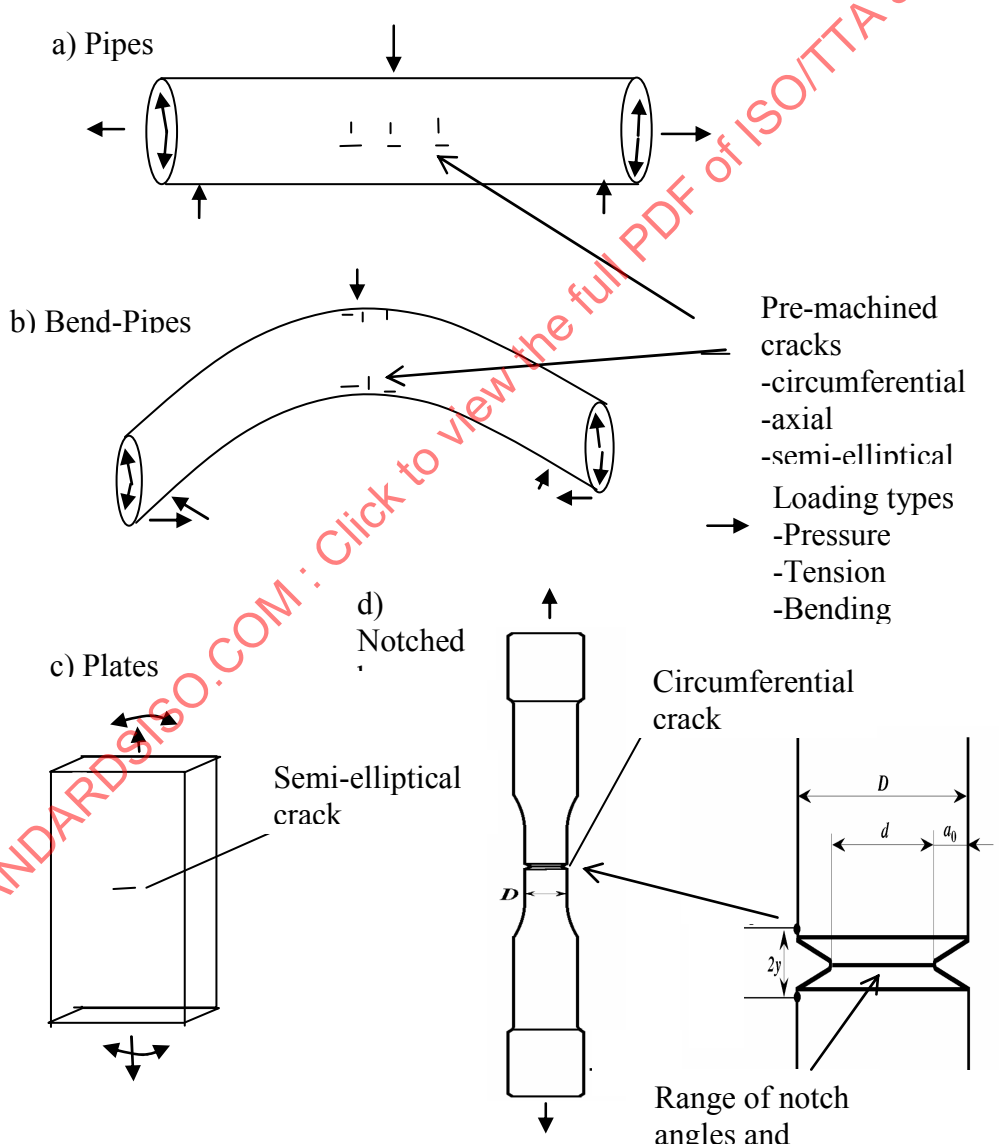

Figure A.I.4: Schematic drawings for the 'feature type' specimens.

It should be noted that there will be a range of dimensional, loading, crack size, shape and materials that would combine in any one 'feature test'. Whilst it is appropriate for the user to follow the present

guidelines both in terms of testing and analysis, set in this document the user should be in a position to validate the relevant parameters for each condition. In Section 14.10 there are quoted specific formulae for the pipe, and plate and notched bar geometries that are quoted. However they are only appropriate for the specific range described and should be validated for other conditions. Therefore parameters such a K, C^*, σ_{ref}, and the creep uniaxial material properties should be derived independently. It is suggested that the user should follow the experimental and analysis methods proposed in this CoP and use appropriate solutions from the literature to derive C^*.

14.10 Fracture Mechanics Functions for Feature Components

The large numbers of feature component and actual component geometries present a very wide range of options which cannot be dealt with individually within this CoP. However it has been found that for most cases the analysis of a semi-elliptical crack in a plate or a pipe would cover most situations that industry is faced with. The loading and boundary conditions will need to be considered in detail for every new case but the principal remains the same. Section 12.2 deals with the derivation of the reference stress estimates of C^* for components using

$$C^* = \sigma_{ref} . \dot{\varepsilon}_{ref} \left(\frac{K}{\sigma_{ref}} \right)^2 \qquad \text{(A.I.93)}$$

and by identifying the appropriate 'global' solution of reference for a particular component and the right stress intensity factor formulae it has been found [34,37-38,69] that conservative estimated of C^* can be derived. The extent or otherwise of the conservatism depends not only on the choice of the formulae but also on the appropriate material properties used. It should also be noted that the value of C^* using Equation (A.I.93) is relatively insensitive to K but is far more sensitive to the reference stress formula chosen.

By highlighting the analysis for a pipe and a plate geometry which have been validated extensively it is suggested that the methodology can be used for other geometries and the results compared to standard laboratory specimens. However it should be noted that a user who wishes to test other geometries needs to compare and verify the data by testing standard C(T) geometries as well, before the results can be used in life assessment cases.

14.10.1 *K solutions for pipes and plates*

In many cases solutions exist for a range of geometries and loading conditions [54-58] which can be accessed quite easily from open databases and available literature. Stress intensity factors for small elliptical cracks in plates and large diameter pipes can be derived from solutions for K due to Raju and Newman [55]. The stress intensity factor has also been derived for elliptical cracks in large plates. There are in the literature several formulae to determine the stress intensity factor. A16 [Commissariat à l'Energie Atomique, 1995][32-33], and BS 7910 [British Standard, 1999] [34], API 579 [35] and R5,R6 [30-31] are all derived from Raju and Newman [55] original calculation which take the form:

$$K_I = F_{K\ Plate} \cdot [\sigma_m + H_{K\ Plate} \cdot \sigma_b] \cdot \sqrt{\frac{\pi \cdot a}{Q_{K\ Plate}}} \qquad \text{(A.I.94)}$$

where the equations for $F_{K\ \text{Plate}}$, $Q_{K\ \text{Plate}}$ and $Q_{K\ \text{Plate}}$ are given in A16 [32] and BS 7910 [m]. As for the pipes, no major differences are expected between the difference stress intensity factor solutions and so the BS 7910 [m] formula has been chosen due to its simplicity to be implemented in any software.

14.10.2 *Reference stress solutions for pipes*

It has been shown previously that although different life assessment codes [30-35] employ the same methods of analysis often different formulae are used to evaluate K and σ_{ref}. Greater sensitivity of C^* and cracking rate to reference stress than to K is expected from Equation (A.I.43). It has also been previously demonstrated that 'global' collapse solution represent best the cracking behavior in pipe components [64]. 'Global' solutions of reference stress are based on collapse of the entire cross-section at the site of a defect. For a semi-elliptical axial defect in a pipe subjected to an internal pressure p, R6 [31] gives:

$$\sigma_{ref\ Pipe} = \frac{p}{\frac{1}{R_e - a} \cdot bate(a,c) + \ln\left(\frac{R_e - a}{R_i}\right)} \qquad \text{(A.I.95)}$$

where *bate(a, c)* is given by :

$$bate(a,c) = \frac{a}{\sqrt{1 + 1.61 \cdot \frac{c^2}{[(R_e - a) \cdot a]}}} \qquad \text{(A.I.96)}$$

where a is crack depth, c is half crack length at the surface and R_i and R_e are the internal and external radii of the pipe, respectively.

Hence by substituting Equation (A.I.95) in Equation (A.I.93) it is possible to derive C^* for pipe components. The additional information that is needed is the stress intensity factor K (see Section 14.10.1) and the uniaxial creep strain rate.

14.10.3 *Reference stress solutions for plates*

Similar to pipes, several reference stress solutions exist for plates. It has been shown, in the past, for small partially penetrating defects in plates subjected to combined tension and bending loading can significantly over-estimate creep crack growth rates [74]. In this present document, a reference stress, which is based on a global collapse mechanism, has been chosen [74] and is expressed as follows:

$$\sigma_{ref\ Plate} = \frac{(\sigma_b + 3 \cdot \gamma \cdot \sigma_m) + \left\{(\sigma_b + 3 \cdot \gamma \cdot \sigma_m) + 9 \cdot \sigma_m^2 \cdot \left[(1-\gamma)^2 + 2 \cdot \gamma \cdot (\alpha - \gamma)\right]\right\}^{1/2}}{3 \cdot \left\{(1-\gamma)^2 + 2 \cdot \gamma \cdot (\alpha - \gamma)\right\}} \qquad \text{(A.I.97)}$$

where $\gamma = (a \cdot c) / (W \cdot l)$ and $\alpha = a / W$ and a is crack depth, c is half crack length at the surface, W is the thickness of the plate and l is the half-width of the plate, respectively.

Hence by substituting Equation (A.I.97) in Equation (A.I.93) it is possible to derive C^* for plate type components. The additional information that is needed is the stress intensity factor K (see Section 14.10.1) and the uniaxial creep strain rate.

14.10.4 *Stress intensity factor K for the round notch bar*

The expression for calculating K for circumferentially notched round bar specimen is given below:

$$K = \frac{1}{2}\sigma_{net}\sqrt{\frac{\pi a d}{D}}\left(1+\frac{1}{2}\lambda+\frac{3}{8}\lambda^2-0.363\lambda^3+0.731\lambda^4\right)\left\{1+0.1\sqrt{\frac{2a}{D}}\left(1-\frac{2a}{D}\right)\right\} \quad \text{(A.I.98)}$$

Where Ligament crack length: $d=D-2a$ and $\lambda=d/D$

The net-section stress σ_{net} for the round notch bar is given below:

$$\sigma_{net} = \frac{P}{\pi\left(\frac{D-2a}{2}\right)^2} \quad \text{(A.I.99)}$$

14.10.5 *C* parameter for the notched bar*

The definition and calculation method of C^* parameter is described in this Section for the round notched bar shown in Figure A.I.4. The magnitude of C^* parameter for circumferentially notched round bar specimen can be determined as follows:

$$C^* = \frac{2n-1}{2n+2}\sigma_{net}\frac{d\Delta}{dt} \quad \text{(A.I.100)}$$

Creep exponent n in the relationship between minimum creep rate and applied stress is obtained from the creep test data using smooth bar specimens in accordance with ISO 204. If creep tests can not be performed the accepted value of n for the specific material taken from literature may be used.

For circumferentially notched bar specimens in tension following equation, therefore, can be used

$$C^* = \frac{2n-1}{2n+2}\frac{P\dot{\Delta}}{\pi\{(D-2a)/2\}^2} \quad \text{(A.I.101)}$$

In Equation (A.I.101), $\dot{\Delta}$ used is the load-line creep displacement rate and is calculated as shown in Section 12.1.

15 APPENDIX II :(TDFAD) K^c_{mat} approach for CCI

Time Dependent Failure Assessment Diagram (TDFAD) approach and the evaluation of a time dependent creep toughness K^c_{mat} used to analyse CCI

15.1 Introduction

Conventional methods for assessing incubation and the early stages of creep crack growth are generally based on the evaluation of parameters including crack opening displacement, δ, and crack tip parameters C^* and $C(t)$ together with experimental data describing creep crack incubation or growth. However, for low temperature fracture, the simplified R6 procedure [31] has been developed, which uses the concept of a Failure Assessment Diagram (FAD) to avoid detailed calculations of crack tip parameters. In recent years, FAD approaches have been extended to the creep regime [60-62] and the high temperature Time Dependent Failure Assessment Diagram (TDFAD) method has now been formally incorporated into the R5 high temperature assessment procedure [30]. A key requirement of TDFAD approaches is the evaluation of time dependent creep toughness, denoted K^c_{mat}, and a number of methods for defining this parameter have been proposed.

15.2 Nomenclature

a_0	Initial crack length
B	Gross specimen thickness
B_e	Effective specimen thickness (defined here *as* B_n *(2 –* B_n/B*)* for consistency with R5 [30])
B_n	Net specimen thickness
C^*	Steady state crack tip parameter
$C(t)$	Transient crack tip parameter
E	Young's modulus
E'	$E/(1-\nu^2)$ for plane strain conditions and E for plane stress conditions
J	J integral
J_e	Elastic J value
J_T	Total J value
K	Stress intensity factor
K^c_{mat}	Material creep toughness corresponding to a given crack extension in a given time
K_r	K / K^c_{mat}
K_r	$\sigma_{ref} / \sigma^c_{0.2}$
L_r^{max}	Cut-off on the R5 TDFAD; minimum of $\sigma_R / \sigma^c_{0.2}$ and $\bar{\sigma} / \sigma_{0.2}$
n	Creep stress exponent
P	Load
U_c	Creep contribution to the total area under the load-displacement curve
U_e	Elastic contribution to the total area under the load-displacement curve

U_p Plastic contribution to the total area under the load-displacement curve

U_T Total area under the load-displacement curve

W Specimen width

δ Crack opening displacement

σ_{n0} Nominal stress (used in the Two Criteria Diagram)

σ_{ref} Reference stress

σ_R Rupture stress for the time and temperature of interest

σ_u Ultimate tensile strength

$\sigma_{0.2}$ 0.2% proof stress; stress corresponding to 0.2% plastic strain

$\sigma_{0.2}^c$ 0.2% inelastic strength; stress corresponding to 0.2% inelastic (plastic plus creep) strain

$\overline{\sigma}$ Short term flow stress $(=(\sigma_{0.2}+\sigma_u)/2)$

ε_{ref} Total strain at the reference stress

ε_{ref}^e Elastic strain at the reference stress

$\varepsilon_{0.2}^e$ Elastic strain at a stress of $\sigma_{0.2}^c$

Δa Crack growth increment

Δ_c Creep component of load-line displacement

Δ_e Elastic component of load-line displacement

Δ_p Plastic component of load-line displacement

Δ_T Total load-line displacement

η Factor relating J to area under the load-displacement curve

15.3 Failure Assessment Diagram

The TDFAD is based on the Option 2 FAD specified in R6 [31] and involves a failure assessment curve relating the two parameters K_r and L_r, which are defined in Equations (A.II.102) and (A.I.103) below, and a cut-off L_r^{max}. For the simplest case of a single primary load acting alone

$$K_r = K / K_{mat}^c \qquad \text{(A.II.102)}$$

where K is the stress intensity factor and K_{mat}^c is the appropriate creep toughness value, and

$$L_r = \sigma_{ref} / \sigma_{0.2}^c \qquad \text{(A.I.103)}$$

where σ_{ref} is the reference stress and $\sigma_{0.2}^c$ is the stress corresponding to 0.2% inelastic (plastic plus creep) strain from the average isochronous stress-strain curve for the temperature and assessment time of interest, see Figure A.II.5. The failure assessment diagram is then defined by the Equations

$$K_r = \left[\frac{E\varepsilon_{ref}}{L_r \sigma^c_{0.2}} + \frac{L_r^3 \sigma^c_{0.2}}{2E\varepsilon_{ref}} \right]^{-1/2}, \quad L_r \le L_r^{\max} \qquad \text{(A.II.104)}$$

$$K_r = 0 \qquad L_r > L_r^{\max} \qquad \text{(A.II.105)}$$

In Equation (A.II.104), E is Young's modulus and ε_{ref} is the total strain from the average isochronous stress-strain curve at the reference stress, $\sigma_{ref} = L_r \sigma^c_{0.2}$, for the appropriate time and temperature. Thus, Equation (A.II.104) enables the TDFAD to be plotted with K_r as a function of L_r, as shown schematically in Figure A.II.6. The cut-off, L_r^{max}, is defined as

$$L_r^{max} = \sigma_R / \sigma^c_{0.2} \qquad \text{(A.II.106)}$$

where σ_R is the rupture stress for the time and temperature of interest. However, for consistency with R6 [31], the value of L_r^{max} should not exceed $\overline{\sigma} / \sigma_{0.2}$ where $\overline{\sigma}$ is the short term flow stress and $\sigma_{0.2}$ is the conventional 0.2% proof stress. As in R6, $\overline{\sigma}$ may be taken as $(\sigma_{0.2} + \sigma_u)/2$ where σ_u is the ultimate tensile strength.

15.4 Materials Data Requirements

A central feature of the TDFAD approach is the definition of an appropriate creep toughness which, when used in conjunction with the failure assessment diagram, ensures that crack growth in the assessment period is less than a value Δa. Creep toughness values may be estimated indirectly from conventional creep crack incubation and growth data or evaluated directly from experimental load versus displacement information. This Section describes the latter direct approach for evaluating creep toughness values.

Direct approaches for determining creep toughness based on experimental load-displacement data can be based on methods used to derive critical J-integral and hence the material toughness, K_{mat}, given in low temperature fracture toughness standards. Consider a load-controlled creep crack growth test conducted on a standard compact tension (C(T)) specimen resulting in a typical load-displacement trace of the form shown in Figure A.II.7. If it is assumed that the amount of crack growth in the test, Δa, is small, the total displacement, Δ_T, may be conveniently partitioned into elastic, plastic and creep components, denoted Δ_e, Δ_p *and* Δ_c, respectively, where

$$\Delta_T = \Delta_e + \Delta_p + \Delta_c \qquad \text{(A.II.107)}$$

Similarly, the total area under the load-displacement curve, U_T, may be conveniently partitioned into elastic, plastic and creep components, denoted U_e, U_p and U_c respectively where

$$U_T = U_e + U_p + U_c \qquad \text{(A.II.108)}$$

The ESIS fracture toughness testing procedure [hh] evaluates experimental total J values, J_T, using the following relationship based on the total area under the load-displacement curve (Noting that fracture toughness testing procedures do not include U_c, the creep contribution to the total area under the load-displacement curve)

$$J_T = \frac{\eta U_T}{B_n(w-a_0)} \qquad \text{(A.II.109)}$$

where W is the specimen width, a_0 is the initial crack length, B_n is the net specimen thickness and

$$\eta = 2 + 0.522(1 - a_0 / w) \qquad \text{(A.II.110)}$$

for C(T) specimens.

The British Standard [s] and ASTM E399 [f] fracture toughness testing procedures adopt an alternative approach for estimating the elastic J value, J_e. This results in the following modified expression for experimental total J values[1]

$$J_T = \frac{K^2}{E'} + \frac{\eta(U_T - U_e)}{B_n(w-a_0)} \qquad \text{(A.II.111)}$$

where K is the stress intensity factor and $E' = E$ for plane stress and $E' = E/(1-\nu^2)$ for plane strain conditions. Values of creep toughness, K^c_{mat}, may then be derived from creep crack growth tests as a function of crack growth increment, Δa, using

$$K^c_{mat} = \sqrt{E' J_T} \qquad \text{(A.II.112)}$$

in conjunction with Equation (A.II.109) or (A.II.111). Thus,

$$K^c_{mat} = \left[\frac{E'\eta U_T}{B_n(w-a_0)}\right]^{1/2} \qquad \text{(A.II.113)}$$

based on the ESIS fracture toughness testing procedure method for evaluating J_T. However, it is considered that the British Standard and ASTM approaches for deriving the elastic contribution to J based on K^2/E' are more robust than the ESIS approach based on U_e, which implicitly assumes that the initial portion of the load-displacement curve accurately reflects the elastic compliance of the specimen. The following expression for direct evaluation of creep toughness from experimental load-displacement information has therefore been proposed

$$K^c_{mat} = \left[K^2 + \frac{E'\eta}{B_n(w-a_0)}\left(U_p + \frac{n}{n+1}U_c\right)\right]^{1/2} \qquad \text{(A.II.114)}$$

where the factor $n/(n+1)$ is required for consistency with standard creep crack growth testing procedures [i] as U_c is defined here as

$$U_c = P\Delta_c \qquad \text{(A.II.115)}$$

where P is the applied load. Therefore Equation (A.II.114) can alternatively be expressed as

$$K_{mat}^{c} = \left[K^2 + \frac{E'\eta U_p}{B_n(w-a_0)} + \frac{n}{n+1}\frac{E'\eta P\Delta_c}{B_n(w-a_0)} \right]^{1/2} \qquad \text{(A.II.116)}$$

which only differs from the Equation (A8.4) of APPENDIX A5 of R5 Volume 4/5 [30] in the use of $E' = E/(1-\nu^2)$ rather than E and the inclusion of an additional second term in Equation (A.II.116) to incorporate the effects of plasticity during loading.

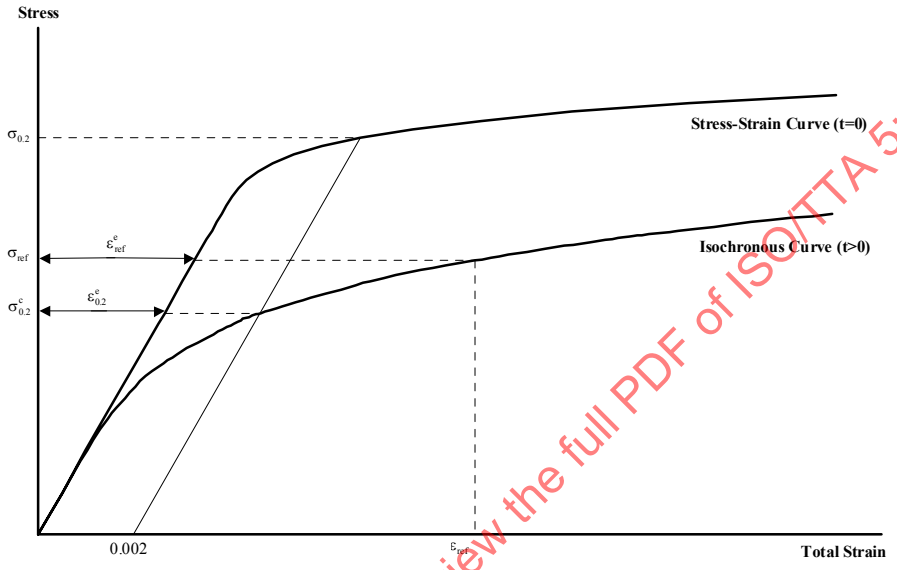

Figure A.II.5: Schematic Isochronous Stress-Strain Curves

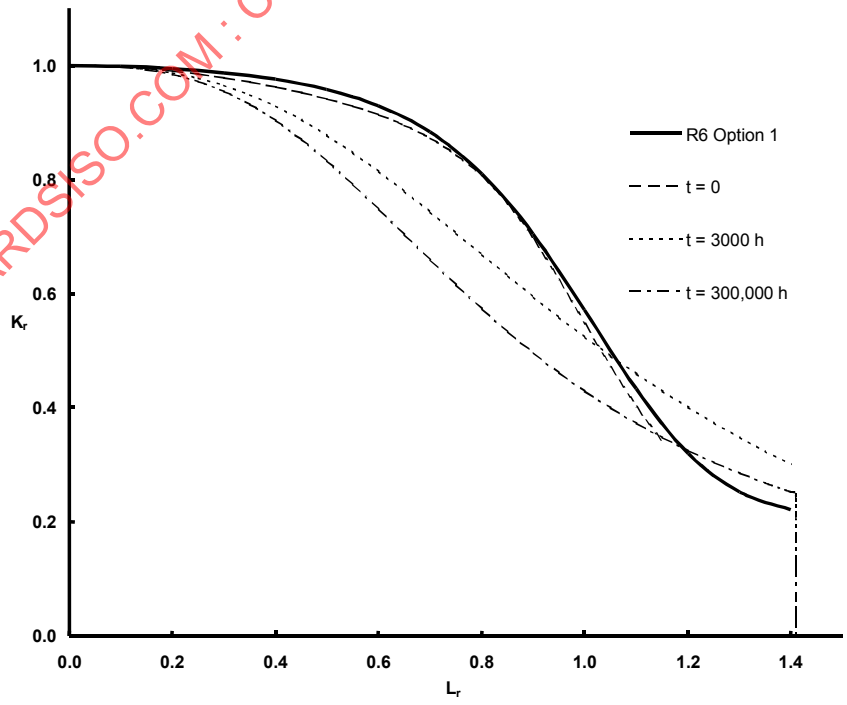

Figure A.II.6: Schematic Failure Assessment Diagrams based on data from an Austenitic Type 316 Steel at 600°C

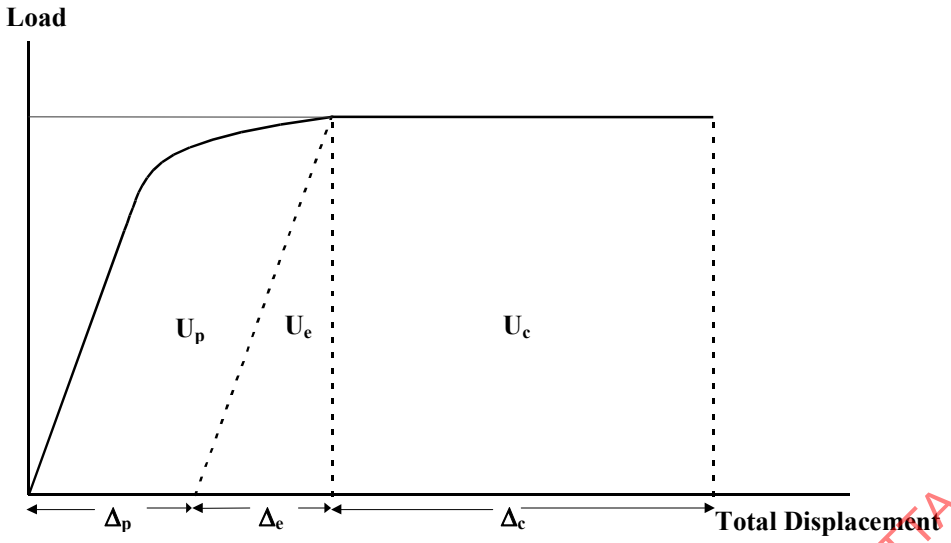

Figure A.II.7: Schematic Load-Displacement Behaviour from a Constant Load Creep Crack Growth Test

16 APPENDIX III: The Q* Parameter

Definition and derivation for the Q^* parameter which is used to describe creep crack growth in creep brittle or ductile materials has been previously published [41-51]. In principle it is suggested that creep crack growth rate can be characterized by the parameter Q^* derived from a combination of thermally activated processes and local crack tip stresses. For the cases in which the steady state crack growth region occupies a large part of life such as in high strengthened materials it has been shown that the steady state CCG rate could be represented as follows ;

$$da/dt = A\ exp(Q^*) \text{ and } \frac{da}{dt} = A\ K_{in}^{m}\ exp\left(-\frac{Q}{RT}\right) \qquad \text{(A.III.117)}$$

where Q is the activation energy, R is the gas constant, and A and m are material constants.

16.1 Symbols and Designations

For the purposes of International Standard the following symbols apply

Symbol	Unit	Designation
a	mm	Crack length
a_0	mm	Initial notch depth before testing
a_f	mm	Actual final crack length when test is completed obtained from fractography measurement
a_{pf}	mm	Predicted final crack length from PD
U	V	Initial value of output voltage
U_0	V	Half distance between out put voltage leads
y	mm	Specimen diameter
D	mm	Ligament crack length: $d=D-2a$
λ	mm	$\lambda=d/D$
P	kN-mm	Applied load
n		Creep exponent of Norton's power creep law
$\delta=\Delta$	mm	Crack opening displacement
$d\delta/dt=d\Delta/dt$	mm/h	Crack opening displacement rate
da/dt	mm/h	Crack growth rate
σ_{net}	MPa	Net section stress
K	MPa√m	Stress intensity factor (mode I)
K_{in}	MPa√m	Initial stress intensity factor when test started
Q	J/Kmol	Activation energy
R	J/Kmol	Gas constant
T	K	Absolute testing temperature

16.2 Scope

This method has been used to evaluate creep crack growth properties in a notched bar containing a circumferential crack (see Figure A.I.4) using an activation energy rate based parameter called Q^*. It has been shown [52,53] in this specific of notched bar specimens that the crack growth rate, *CCG* rate can be evaluated and compared in terms of the fracture mechanical parameter C^*, Q^* and K. The test procedure follows that of the other geometries shown in Section A1.1. It should be noted that tests at different temperatures are needed in order to derive the activation energies needed to evaluate Q^*.

16.3 Specimen Geometry

The shape of the notch bar specimen is shown in Figure A.I.4. Except for the notch the dimensions shall meet the requirement of creep test of smooth bar specimen in ISO 204.

16.4 Guideline for Calculation of the Q^* parameter

16.4.1 Crack Growth Analysis

Q^* parameter for structural strengthened materials such as γ' Ni-base superalloys, 9-12Cr tempered martensite steel, or under multi-axial stress condition such as circular notched bar specimen, producing creep brittle conditions at the crack tip, is given as follows [15,50-53]:

$$Q^* = m\,log\left(\frac{K_{in}}{K_0}\right) - \frac{Q}{RT} \qquad \text{(A.III.118)}$$

where, Q is the activation energy, K_{in} is the initial stress intensity factor, K_0 (normalizing factor) is $1\text{MPam}^{1/2}$, m is power coefficient value of K_{in} in the equation of creep crack growth rate. Creep crack growth rate is the given by

$$\frac{da}{dt} = A\exp(Q^*) \qquad \text{(A.III.119)}$$

and

$$\frac{da}{dt} = A K_{in}^{m} \exp\left(-\frac{Q}{RT}\right) \qquad \text{(A.III.120)}$$

by integrating Equation (A.III.120) creep crack growth life is given by :

$$t_f = \frac{C}{A} exp(\frac{Q}{RT}) \frac{1}{K_{in}^{m}} \qquad \text{(A.III.121)}$$

and

$$ln\,K_{in} = \frac{1}{m} ln\frac{C}{A} - \frac{1}{m}\left(ln\,t_f - \frac{Q}{RT}\right) \qquad \text{(A.III.122)}$$